AD-A187 455 A FINITE ELEMENT ANALYSIS OF ADHESIVELY BONDED COMPOSITE JOINTS INCLUDING..(U) VIRGINIA TECH CENTER FOR ADHESION SCIENCE BLACKSBURG S ROY ET AL. OCT 87 CAS/ESM-87-9 N00014-82-K-0185 F/G 13/5 1/1

UNCLASSIFIED NL

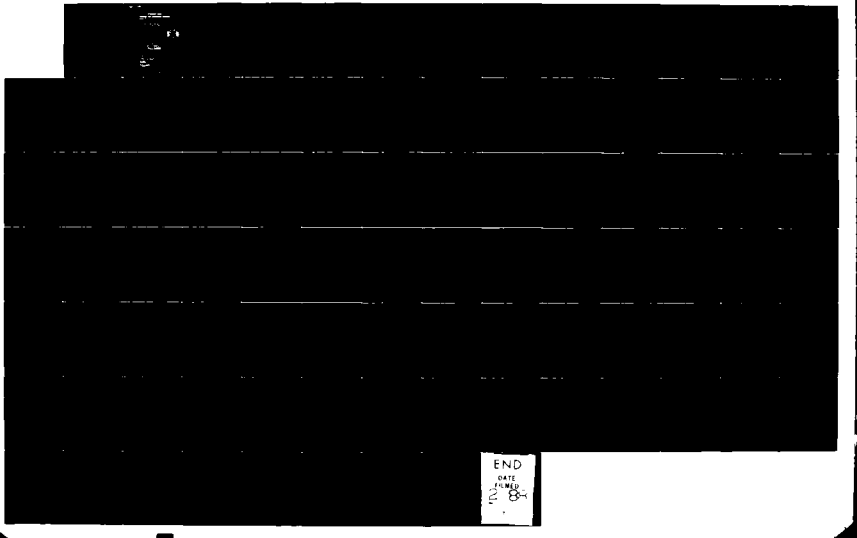

END
DATE FILMED
1-88
DTIC

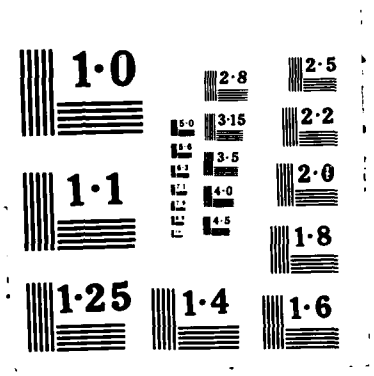
1·0
1·1
1·25
1·4
1·6
2·8
3·15
3·5
4·0
4·5
5·0
2·5
2·2
2·0
1·8

VIRGINIA TECH
CENTER FOR ADHESION SCIENCE

October 1987

A FINITE ELEMENT ANALYSIS OF ADHESIVELY BONDED COMPOSITE JOINTS INCLUDING GEOMETRIC NONLINEARITY, NONLINEAR VISCOELASTICITY, MOISTURE DIFFUSION AND RELATED FAILURE

INTERIM REPORT

S. ROY, RESEARCH ASSISTANT
DEPARTMENT OF ENGINEERING SCIENCE AND MECHANICS

J. N. REDDY, PROFESSOR
DEPARTMENT OF ENGINEERING SCIENCE AND MECHANICS

Support for this work was provided by the Office of Naval
Research (Contract No. N00014-82-K-0183)
Dr. Yapa Rajapakse, Jr., Project Monitor

SECURITY CLASSIFICATION OF THIS PAGE (When Data Entered)

REPORT DOCUMENTATION PAGE	READ INSTRUCTIONS BEFORE COMPLETING FORM
1 REPORT NUMBER	2. GOVT ACCESSION NO. AD-A187455 / 3. RECIPIENT'S CATALOG NUMBER
4. TITLE (and Subtitle) A FINITE ELEMENT ANALYSIS OF ADHESIVELY BONDED COMPOSITE JOINTS INCLUDING GEOMETRIC NONLINEARITY, NONLINEAR VISCOELASTICITY, MOISTURE DIFFUSION AND DELAYED FAILURE	5. TYPE OF REPORT & PERIOD COVERED Interim
	6 PERFORMING ORG. REPORT NUMBER VPI-E-87-21; CAS/ESM-87-9
7. AUTHOR(s) S. Roy and J. N. Reddy	8. CONTRACT OR GRANT NUMBER(s) N00014-82-K-0185
9. PERFORMING ORGANIZATION NAME AND ADDRESS Virginia Polytechnic Institute and State University Blacksburg, Virginia 24061	10. PROGRAM ELEMENT, PROJECT, TASK AREA & WORK UNIT NUMBERS NR 039-229/8-12-83 (431)
11. CONTROLLING OFFICE NAME AND ADDRESS Office of Naval Research Mechanics Division (Code 430) 800 N. Quincy St., Arlington, VA 22217	12 REPORT DATE October 1987
	13. NUMBER OF PAGES 86 + 3
14 MONITORING AGENCY NAME & ADDRESS(if different from Controlling Office)	15 SECURITY CLASS. (of this report) UNCLASSIFIED
	15a. DECLASSIFICATION/DOWNGRADING SCHEDULE

16. DISTRIBUTION STATEMENT (of this Report)

This document has been approved for public release and sale; distribution unlimited.

17. DISTRIBUTION STATEMENT (of the abstract entered in Block 20, if different from Report)

18. SUPPLEMENTARY NOTES

19. KEY WORDS (Continue on reverse side if necessary and identify by block number)

Adhesive joints, bonded joints, finite element analysis, composite joints, moisture diffusion, delayed failure, nonlinear viscoelasticity, numerical results.

20. ABSTRACT (Continue on reverse side if necessary and identify by block number)

A two-dimensional finite-element computational procedure is developed for an analysis of adhesively bonded joints with nonlinear viscoelasticity, moisture diffusion and delayed failure models. Effect of temperature and stress level on the viscoelastic response is taken into account by a nonlinear shift factor definition, and penetrant sorption is accounted via a nonlinear Fickean diffusion model in which the diffusion coefficient is dependent on the penetrant concentration and dilatational strain. A delayed failure criterion based on the Reiner-Weisenberg failure theory is also included. Several example problems are

DD FORM 1 JAN 73 1473 EDITION OF 1 NOV 65 IS OBSOLETE UNCLASSIFIED

SECURITY CLASSIFICATION OF THIS PAGE (When Data Entered)

(abstract continue from Item 20)

included. The results are discussed in view of the analytical or experimental results available in the literature. The finite element analysis results are in found to be in good agreement.

Department of the Navy
OFFICE OF NAVAL RESEARCH
Materials Division
Arlington, Virginia 22217

Contract N00014-82-K-0185
Task No. NR 039-229/8-12-83 (430)
INTERIM REPORT

Research Report No. VPI-E-87.21

A FINITE ELEMENT ANALYSIS OF ADHESIVELY BONDED COMPOSITE JOINTS INCLUDING GEOMETRIC NONLINEARITY, NONLINEAR VISCOELASTICITY, MOISTURE DIFFUSION AND DELAYED FAILURE

by

S. Roy and J. N. Reddy
Department of Engineering Science and Mechanics
Virginia Polytechnic Institute and State University
Blacksburg, VA 24061

October 1987

Blacksburg, Virginia

A FINITE ELEMENT ANALYSIS OF ADHESIVELY BONDED COMPOSITE JOINTS GEOMETRIC NONLINEARITY, NONLINEAR VISCOELASTICITY, MOISTURE DIFFUSION AND DELAYED FAILURE

by

S. Roy* and J. N. Reddy**
Department of Engineering Science and Mechanics
Virginia Polytechnic Institute and State University
Blacksburg, Virginia 24061

SUMMARY

A two-dimensional finite-element computational procedure is developed for the accurate analysis of the strains and stresses in adhesively bonded joints. The adhesive layer is modeled using Schapery's nonlinear single integral constitutive law for uniaxial and multiaxial states of stress. Effect of temperature and stress level on the viscoelastic response is taken into account by a nonlinear shift factor definition. Penetrant sorption is accounted for by a nonlinear Fickean diffusion model in which the diffusion coefficient is dependent on the penetrant concentration and the dilatational strain. A delayed failure criterion based on the Reiner-Weisenberg failure theory has also been implemented in the finite element code. The applicability of the proposed models is demonstrated by several numerical examples.

---

* Graduate Research Assistant

** Clifton C. Garvin Professor of Engineering

TABLE OF CONTENTS

1. INTRODUCTION

1.1 Preliminary Comments

During the last two years of research for the office of Naval Research a finite-element computer program, NOVA, has been under continuous development for an accurate analysis of adhesively bonded joints (see [1,2]). The finite element program NOVA uses linearly elastic elements to model the adherends. The adherends can be represented as isotropic, orthotropic or laminated composite materials. The large displacements and rotations experienced by the adherends in many types of loading are accounted for by the updated Lagrangian description of motion. The adhesive layer is modeled using a special element that employs a multi-axial extension of Schapery's nonlinear single integral stress-strain law as the constitutive equation. The finite element formulation based on the updated Lagrangian incremental equations is presented in detail in [1,2]. The element library contains an eight noded isoparametric element which employs quadratic interpolation functions to represent the displacement field as well as element geometry. The program can be used to conduct plane stress, plane strain, or axisymmetric analysis of an adhesively bonded structure subject to a time varying thermal and mechanical loading. The program is modified recently to include a nonlinear Fickean moisture diffusion model and a energy-based delayed failure criterion. This report describes the theory, finite element formulation and applications of NOVA to moisture diffusion and delayed failure problems.

1.2. A Review of the Literature

Over the years several time-dependent failure criteria have been proposed for predicting yield and fracture of polymeric materials. Nagdhi and Murch [3] and Crochet [4] have used a modified von Mises criteria for viscoelastic materials by assuming that the radius of the yield surface depends upon the strain history. An energy based delayed failure criterion for polymeric materials subjected to isothermal creep was developed by Reiner and Weissenberg [5]. According to this theory, failure occurs when the stored deviatoric strain energy in a viscoelastic material reaches a certain maximum value called the resilience, which is a material constant. Brüller [6] and Hiel et al. [7] applied the Reiner-Weisenberg failure criterion to various viscoelastic materials, including composite laminates, and obtained good agreement with experimental observations.

It is now well known that moisture diffusion can have a significant effect on the stress field within an adhesive layer in a bond. Weitsman [8] used a variational method coupled with Fickean diffusion law to study the interfacial stresses in viscoelastic adhesive-layers due to moisture sorption. From the results of this uncoupled linear thermoelastic analysis, he concluded that the location of the maximum interfacial tensile stress depends on the geometry of the joint as well as the progress of the diffusion process within the joint. Weitsman [9] used the correspondence principle to generate a linear viscoelastic solution from the linear elastic analysis of moisture sorption within an adhesive layer. He observed that the viscoelastic analysis predicts detrimental effects due to stress reversals caused by fluctuations in relative humidity, that are not predicted in an elastic analysis.

However, he acknowledged the omission of the effect of moisture content on the viscoelastic response of the resins in his analysis.

Tobing, et al. [10] used the finite element method to study the micro-mechanical effect of moisture sorption in graphite-epoxy composites. Using a constitutive equation based on the Flory-Huggins lattice model for polymer solvent interactions, they concluded that the stresses at the graphite-epoxy interface have a strong dependence on moisture content, fiber spacing, and applied load.

Yaniv and Ishai [11] developed a linear viscoelastic closed form solution as well as a nonlinear finite element solution algorithm to study the hygrothermal effects in a bonded fiber-reinforced plastic/aluminum system. The linear solution was used for short-term predictions at low strain levels, whereas the finite element solution was used for long term predictions in which geometric and material nonlinearities were taken into account. The authors observed that the presence of moisture tends to considerably reduce the stress level in the adhesive layer and may lead to significant variation in the time-dependent deformation of the test specimen as compared to the dry state.

In the references cited above, various authors have underscored the effect of moisture content on the viscoelastic response of the test specimen. However, the effect of the viscoelastic stress field on the diffusion coefficient was not considered. Lefebvre et al. [12] extended the free volume concept to define a diffusion coefficient that is a function of temperature, dilatational strain and solvent concentration. The proposed nonlinear diffusion model showed good predictive capability for different values of temperature and moisture conentrations. They concluded that in order to obtain an accurate

solution for the hygrothermal effects within an adhesive bond, the nonlinear diffusion problem needs to be solved in conjunction with the nonlinear viscoelastic boundary-value problem until convergence is achieved.

2. NONLINEAR VISCOELASTIC FORMULATION

2.1 Introduction

A thermodynamically consistent theory for a single integral representation of nonlinear viscoelasticity was first proposed by Schapery [13]. The law can be derived from fundamental principles using the concepts of irreversible thermodynamics. A comprehensive review of the thermodynamics basis of Schapery's theory has been presented by Hiel et al. [14].

The following two sections deal with the review and application of Schapery's single integral constitutive law to problems with uniaxial and multiaxial states of stress, respectively. The constitutive equations thus obtained are suitable for non-linear viscoelastic finite element analysis.

2.2 Uniaxial Stress State

The uniaxial nonlinear viscoelastic constitutive equation of Schapery [13] can be written for an isotropic material as,

$$\varepsilon^t = g_o^t \sigma^t D_o + g_1^t \int_0^t \Delta D(\psi^t - \psi^s) \frac{d}{ds} [g_2^s \sigma^s] ds. \qquad (2.1)$$

In Eq. (2.1), ε^t represents uniaxial kinematic strain at current time t, σ^t is the Cauchy stress at time t, D_o is the instantaneous elastic compliance and $\Delta D(\psi)$ is a transient creep compliance function. Superscript, t, denotes current time. The factor g_o^t defines stress and

temperature effects on the instantaneous elastic compliance and is a measure of state dependent reduction (or increase) in stiffness, $g_o^t = g_o(\sigma,T)$. Transient (or creep) compliance factor g_1^t has similar meaning, operating on the creep compliance component. The factor g_2^t accounts for the influence of load rate on creep, and depends on stress and temperature. The function ψ^t represents a reduced time scale parameter defined by,

$$\psi^t = \int_0^t (a_{\sigma T}^s)^{-1} ds, \tag{2.2}$$

where $a_{\sigma T}^s$ is a time scale 'shift factor'. For thermorheologically simple materials, $a = a(T)$ is a function of temperature T only. This function modifies, in general, viscoelastic response as a function of temperature and stress. Mathematically, $a_{\sigma T}^s$ shifts the creep data parallel to the time axis relative to a master curve for creep strain versus time. In this model, four material parameters (g_o^t, g_1^t, g_2^t and a^t) are available to characterize the nonlinear behavior instead of only one with the time scale shifting procedure of Knauss and Emri [15].

The transient creep compliance, $\Delta D(\psi)$, can be expressed in exponential form as,

$$\Delta D(\psi) = \sum_r D_r [1 - e^{-\lambda_r \psi^t}], \tag{2.3}$$

where D_r and λ_r are constants. Substitution of Eq. (2.3) in Eq. (2.1) gives,

$$\varepsilon^t = g_o^t D_o \sigma^t + g_1^t \int_0^t \sum_r D_r [1 - e^{-\lambda_r (\psi^t - \psi^s)}] \frac{d}{ds} [g_2^s \sigma^s] ds. \tag{2.4}$$

Letting the product $g_2^s \sigma^s$ be expressed as G^s and simplifying the integrand on the right hand side of Eq. (2.4) yields,

$$\varepsilon^t = g_o^t D_o \sigma^t + g_1^t \sum_r D_r \int_0^t \frac{d}{ds} G^s ds - g_1^t \sum_r D_r \int_0^t e^{-\lambda_r(\psi^t - \psi^s)} \frac{dG^s}{ds} ds. \tag{2.5}$$

The third integration term on the right hand side of Eq. (2.5) is now separated into two parts, the first part having limits from zero to $(t - \Delta t)$ and the second integral spanning only the current load step, i.e., from $(t - \Delta t)$ to t. Hence,

$$\int_0^t e^{-\lambda_r(\psi^t - \psi^s)} \frac{dG^s}{ds} ds = \int_0^{t-\Delta t} e^{-\lambda_r(\psi^t - \psi^s)} \frac{dG^s}{ds} ds + \int_{t-\Delta t}^t e^{-\lambda_r(\psi^t - \psi^s)} \frac{dG^s}{ds} ds. \tag{2.6}$$

The first term on the right hand side of Eq. (2.6) can be rewritten as,

$$\int_0^{t-\Delta t} e^{-\lambda_r(\psi^t - \psi^s)} \frac{dG^s}{ds} ds = e^{-\lambda_r \Delta \psi^t} q_r^{t-\Delta t}, \tag{2.7}$$

where

$$\Delta \psi^t = \psi^t - \psi^{t-\Delta t} \tag{2.8}$$

$$q_r^{t-\Delta t} = \int_0^{t-\Delta t} e^{-\lambda_r(\psi^{t-\Delta t} - \psi^s)} \frac{dG^s}{ds} ds. \tag{2.9}$$

The second integral on the right hand side of Eq. (2.6) is now integrated by parts. To carry out the integration, it is assumed that G^t varies linearly over the current time step Δt. Hence,

$$\int_{t-\Delta t}^t e^{-\lambda_r(\psi^t - \psi^s)} \frac{dG^s}{ds} ds = \frac{dG^s}{ds} \frac{e^{-\lambda_r(\psi^t - \psi^s)}}{\lambda_r} \Bigg|_{t-\Delta t}^t - \int_{t-\Delta t}^t \frac{d^2 G^s}{ds^2} \frac{e^{-\lambda_r(\psi^t - \psi^s)}}{\lambda_r} ds$$

$$= \frac{dG^t}{dt} \left[\frac{1 - e^{-\lambda_r \Delta\psi^t}}{\lambda_r}\right]. \qquad (2.10)$$

In arriving at the second step, it is assumed that G^s is linear and hence its second derivative is zero. Since G^t has been assumed to be a linear function of time over the current load step, we can write

$$\frac{dG^t}{dt} = \frac{G^t - G^{t-\Delta t}}{\Delta\psi^t}. \qquad (2.11)$$

Substitution of Eq. (2.11) into Eq. (2.10) gives

$$\int_{t-\Delta t}^{t} e^{-\lambda_r(\psi^t - \psi^s)} \frac{dG^s}{ds}\, ds = [G^t - G^{t-\Delta t}]\beta_r^t, \qquad (2.12)$$

where,

$$\beta_r^t = \frac{1 - e^{-\lambda_r \Delta\psi^t}}{\lambda_r \Delta\psi^t}. \qquad (2.13)$$

Substituting Eq. (2.9) and Eq. (2.12) back into Eq. (2.5), and writing $G^t = g_2^t \sigma^t$, one obtains

$$\varepsilon^t = [g_o^t D_o + g_1^t g_2^t \sum_r D_r - g_1^t g_2^t \sum_r D_r \beta_r^t]\sigma^t + g_1^t \sum_r D_r [g_2^{t-\Delta t} \beta_r^t \sigma^{t-\Delta t} - e^{-\lambda_r \Delta\psi^t} q_r^{t-\Delta t}]. \qquad (2.14)$$

Defining instantaneous compliance D_I^t as the compliance term multiplying the instantaneous stress σ^t, and the remaining terms in Eq. (2.14) as hereditary strains E^t, one can write

$$\varepsilon^t = D_I^t \sigma^t + E^t \equiv F(\sigma), \qquad (2.15)$$

where

$$D_I^t = g_o^t D_o^t + g_1^t g_2^t \sum_r D_r - g_1^t g_2^t \sum_r D_r \beta_r^t \qquad (2.16)$$

$$E^t = g_1^t\{\sum_r D_r[g_2^{t-\Delta t}\beta_r^t\sigma^{t-\Delta t} - e^{-\lambda_r\Delta\psi^t} q_r^{t-\Delta t}]\}. \qquad (2.17)$$

Equation (2.15) expresses Schapery's single integral constitutive law in terms of a stress operator that includes instantaneous compliance and hereditary strains.

It is to be noted that the term $q_r^{t-\Delta t}$ in Eq. (2.17) is the r^{th} component of the hereditary integral series at the end of the previous load step (i.e. at time equals t - Δt). The expression for the hereditary integral at the end of the current load step (i.e. at time t) can be derived in the form of a recurrence formula. From Eq. (2.9), one can write

$$q_r^t = \int_0^t e^{-\lambda_r(\psi^t-\psi^s)} \frac{dG^s}{ds} ds$$

$$= \int_0^{t-\Delta t} e^{-\lambda_r(\psi^t-\psi^s)} \frac{dG^s}{ds} ds + \int_{t-\Delta t}^t e^{-\lambda_r(\psi^t-\psi^s)} \frac{dG^s}{ds} ds. \qquad (2.18)$$

Using the results from Eqs. (2.9) and (2.12), the above equation can be reduced to

$$q_r^t = e^{-\lambda_r\Delta\psi^t} q_r^{t-\Delta t} + [g_2^t\sigma^t - g_2^{t-\Delta t}\sigma^{t-\Delta t}]\beta_r^t, \qquad (2.19)$$

where β_r^t is defined by Eq. (2.13).

2.3 Multiaxial Stress State

For a thermorheologically simple anisotropic viscoelastic material under a multiaxial state of stress, the constitutive law proposed by Schapery [13] is,

$$e_{ij} = -\frac{\partial G_R}{\partial\sigma_{ij}} + \frac{\partial\hat{\sigma}_{mn}}{\partial\sigma_{ij}} \Delta\hat{e}_{mn} \qquad (2.20)$$

$$\Delta\hat{e}_{mn} = \int_{-\infty}^{t} \Delta S_{mn}^{ij}(\psi^t - \psi^\tau) \frac{\partial}{\partial\tau} (\hat{\sigma}_{ij}/a_G) d\tau \qquad (2.21)$$

where e_{ij} and σ_{ij} are the components of the strain and stress tensors, respectively; G_R is the Gibbs free energy, $\hat{\sigma}_{ij}$ and ΔS_{mn}^{ij} are the components of the second and fourth order material property tensors, respectively; and a_G is a material kernel function defined in [13]. The quantities G_R, a_G and $\hat{\sigma}_{mn}$ are, in general, functions of ten variables, σ_{ij} and temperature T. Note that all repeated indices in Eqs. (2.20) and (2.21) are to be summed over their range (1,2,3).

Due to the complex nature of Eq. (2.20) it is not possible to determine the material properties in this equation from the uniaxial tests outlined in [13]. However, it is possible to construct a set of small strain, three-dimensional constitutive equations from Eq. (2.20), which is consistent with the thermodynamic theory in [13] and yet enables all properties to be evaluated from uniaxial tests. The assumptions which need to be made for this purpose are as follows:

(a) The Gibb's free energy G_R is a quadratic function of stress,

(b) $\hat{\sigma}_{ij} = \sigma_{ij}$ (2.22)

When the free energy G_R is a quadratic function of stress one has

$$-\frac{\partial G_R}{\partial \sigma_{ij}} = S_{ij}^{mn}(0)\sigma_{mn}, \qquad (2.23)$$

where $S_{ij}^{mn}(0)$ are the instantaneous components of the linear viscoelastic creep compliance tensor. Equation (2.23) implies that the initial response of the material is linearly elastic under suddenly applied stresses, which is often the case for metals and plastics.

The second assumption, on the other hand, leads to the linearization of the coefficient of the transient term in Eq. (2.20).

Mathematically, this is given by,

$$\frac{\partial \hat{\sigma}_{mn}}{\partial \sigma_{ij}} = \begin{cases} 1, & \text{if } i = m \text{ and } j = n \\ 0, & \text{if } i \neq m \text{ and } j \neq n \end{cases} \tag{2.24}$$

Equation (2.24) implies that the jump in strain due to load application equals the jump when the load is removed. This behavior is exhibited by some types of plastics [16].

Substituting Eqs. (2.23) and (2.24) in Eqs. (2.20) and (2.21), one obtains

$$e_{ij}^t = S_{ij}^{mn}(0)\sigma_{mn} + \Delta\hat{e}_{ij}^t \tag{2.25}$$

$$\Delta\hat{e}_{ij}^t = \int_{-\infty}^{t} \Delta S_{ij}^{mn}(\psi^t - \psi^\tau) \frac{\partial}{\partial \tau} (g_2^\tau \sigma_{mn}^\tau) d\tau, \tag{2.26}$$

where $g_2^\tau = 1/a_G^\tau$. Equation (2.25) is a set of three-dimensional constitutive equations for anisostropic viscoelastic materials which includes the nonlinear functions g_2^t and $a_{\sigma T}^t$ appearing in the uniaxial relations (2.1) and (2.2). Note that the functions g_2^t and $a_{\sigma T}^t$ are expressed as a function of the octrahedral shear stress.

For a homogeneous isotropic nonlinear viscoelastic material, Eq. (2.24) reduces to the form presented by Schapery ([13] and [16]),

$$e_{ij}^t = \{J\}\{g_2^t \sigma_{ij}^t\} + \{D - J\}\{g_2^t \sigma_{mm}^t\}\delta_{ij}, \tag{2.27}$$

where

$$\{J\}\{g_2^t \sigma_{ij}^t\} = J(0)\sigma_{ij} + \int_0^t \Delta J(\psi^t - \psi^\tau) \frac{\partial}{\partial \tau} (g_2^\tau \sigma_{ij}^\tau) d\tau \tag{2.28}$$

$$\{D - J\}\{g_2^t \sigma_{mm}^t\} = [D(0) - J(0)]\sigma_{mm}^t + \int_0^t [\Delta D(\psi^t - \psi^\tau)$$

$$- \Delta J(\psi^t - \psi^\tau)] \frac{\partial}{\partial \tau} (g_2^\tau \sigma_{mm}^\tau) d\tau \tag{2.29}$$

$$\psi^t - \psi^\tau = \int_\tau^t (a^s_{\sigma T})^{-1} ds \,. \tag{2.30}$$

Expanding Eq. (2.27) term by term for the strains, one has

$$e^t_{11} = \{D\}\{g^t_2 \sigma^t_{11}\} + \{D - J\}\{g^t_2 \sigma^t_{22}\} + \{D - J\}\{g^t_2 \sigma^t_{33}\} \,. \tag{2.31a}$$

Similarly,

$$e^t_{22} = \{D - J\}\{g^t_2 \sigma^t_{11}\} + \{D\}\{g^t_2 \sigma^t_{22}\} + \{D - J\}\{g^t_2 \sigma^t_{33}\}$$

$$\gamma^t_{12} = 2\{J\}\{g^t_2 \sigma^t_{12}\}$$

$$e^t_{33} = \{D - J\}\{g^t_2 \sigma^t_{11}\} + \{D - J\}\{g^t_2 \sigma^t_{22}\} + \{D\}\{g^t_2 \sigma^t_{33}\} \,. \tag{2.31b}$$

The transient components of the creep and shear compliances can be written in the form of the Prony series as,

$$\Delta D(\cdot) = \sum_r D_r [1 - e^{-\lambda_r \cdot}]$$

$$\Delta J(\cdot) = \sum_r J_r [1 - e^{-\cdot r \cdot}] \,, \tag{2.32}$$

where λ_r and r are the reciprocal of the retardation times in creep and shear respectively. Also, let,

$$D(0) = D_0$$

$$J(0) = J_0 \tag{2.33}$$

Considering a term of the form $\{D\}\{g^t_2 \sigma^t_{ij}\}$ in Eq. (2.31) and substituting Eqs. (2.32) into Eq. (2.33) gives,

$$\{D\}\{g^t_2 \sigma^t_{ij}\} = D_o \sigma^t_{ij} + \int_0^t \sum_r D_r [1 - e^{-\lambda_r (\psi^t - \psi^\tau)}] \frac{d}{d\tau} [g^\tau_2 \sigma^\tau_{ij}] d\tau \tag{2.34}$$

Recognizing that Eq. (2.34) is similar in appearance to Eq. (2.6) and making use of the results derived in Section 2.2, one obtains

$$\{D\}\{g_2^t \sigma_{ij}^t\} = D_I^t \sigma_{ij}^t + Q_{ij}^t, \tag{2.35}$$

where D_I^t is the instantaneous creep compliance function at time t,

$$D_I^t = D_o + g_2^t \sum_r D_r(1 - \beta_r^t),$$

Q_{ij}^t are the hereditary strain components due to tensile creep at time t,

$$Q_{ij}^t = \sum_r [g_2^{t-\Delta t} \beta_r^t \sigma_{ij}^{t-\Delta t} - e^{-\lambda_r \Delta\psi^t} q_{r,ij}^{t-\Delta t}]$$

$$\beta_r^t = \frac{1 - e^{-\lambda_r \Delta\psi^t}}{\lambda_r \Delta\psi^t}$$

and, $q_{r,ij}^t$ are components of the hereditary integral given by the recurrence formula,

$$q_{r,ij}^t = e^{-\lambda_r \Delta\psi^t} q_{r,ij}^{t-\Delta t} + [g_2^t \sigma_{ij}^t - g_2^{t-\Delta t} \sigma_{ij}^{t-\Delta t}] \beta_r^t .$$

Similarly, a term of the form $\{J\}\{g_2^t \sigma_{ij}^t\}$ in Eq. (2.31a) can be expressed as,

$$\{J\}\{g_2^t \sigma_{ij}^t\} = J_I^t \sigma_{ij}^t + P_{ij}^t, \tag{2.36}$$

where, J_I^t is the instantaneous shear compliance function at time t,

$$J_I^t = J_o + g_2^t \sum_r J_r(1 - \gamma_r^t),$$

P_{ij}^t are the hereditary strain components due to shear at time t,

$$P_{ij}^t = \sum_r [g_2^{t-\Delta t} \gamma_r^t \sigma_{ij}^{t-\Delta t} - e^{-\eta_r \Delta\psi^t} p_{r,ij}^{t-\Delta t}]$$

$$\gamma_r^t = \frac{1 - e^{-\eta_r \Delta\psi^t}}{\eta_r \Delta\psi^t}$$

and, $p^t_{r,ij}$ are components of the hereditary integral given by the recurrence formula

$$p^t_{r,ij} = e^{-\eta_r \Delta\psi^t} p^{t-\Delta t}_{r,ij} + [g_2^t \sigma^t_{ij} - g_2^{t-\Delta t} \sigma^{t-\Delta t}_{ij}] \Gamma^t_r$$

Substituting Eqs. (2.35) and (2.36) in Eqs. (2.31) and dropping superscripts, one obtains

$$e_{11} = D_1 \sigma_{11} + (D_I - J_I)\sigma_{22} + (D_I - J_I)\sigma_{33} + H_{11}$$

$$e_{22} = (D_I - J_I)\sigma_{11} + D_I \sigma_{22} + (D_I - J_I)\sigma_{33} + H_{22}$$

$$\gamma_{12} = 2J_I \sigma_{12} + H_{12}$$

$$e_{33} = (D_I - J_I)\sigma_{11} + (D_I - J_I)\sigma_{22} + D_I \sigma_{33} + H_{33}, \qquad (2.37)$$

where

$$H_{11} = Q_{11} + Q_{22} + Q_{33} - P_{22} - P_{33}$$

$$H_{22} = Q_{11} + Q_{22} + Q_{33} - P_{11} - P_{33}$$

$$H_{12} = 2P_{12}$$

$$H_{33} = Q_{11} + Q_{22} + Q_{33} - P_{11} - P_{22}. \qquad (2.38)$$

Equation (2.37) can be expressed in matrix form as

$$\{e\} = [N]\{\sigma\} + \{H\}. \qquad (2.39)$$

Note that the left hand side of Eq. (2.39) is a vector containing the algebraic difference of kinematic strains $\{\varepsilon\}$ and dilatational strains $\{\delta_{ij}\theta\}$,

$$\{e\}^T = \{(\varepsilon_{11} - \theta),(\varepsilon_{22} - \theta),\gamma_{12},(\varepsilon_{33} - \theta)\}, \qquad (2.40)$$

while $\{\sigma\}$ contains four components of Cauchy stress,

$$\{\sigma\}^T = \{\sigma_{11},\sigma_{22},\sigma_{12},\sigma_{33}\},$$

and $\{H\}$ is a vector of hereditary strains given by,

$$\{H\}^T = \{H_{11},H_{22},H_{12},H_{33}\}.$$

The matrix $[N]$ is a 4 x 4 coefficient matrix given by,

$$[N] = \begin{bmatrix} D_I & (D_I-J_I) & 0 & (D_I-J_I) \\ (D_I-J_I) & D_I & 0 & (D_I-J_I) \\ 0 & 0 & 2J_I & 0 \\ (D_I-J_I) & (D_I-J_I) & 0 & D_I \end{bmatrix}.$$

Pre-multiplying Eq. (2.39) by $[N]^{-1}$, an explicit expression for stresses in terms of strains is obtained:

$$\{\sigma\} = [M](\{e\} - \{H\}) \ , \ [M] = [N]^{-1}. \qquad (2.41)$$

Equation (2.41) provides a general viscoelastic constitutive relation that can be applied to either plane stress, plane strain or axisymmetric problems. For plane strain, the out-of-plane strain component e_{33} is identically zero. The corresponding stress component, σ_{33}, may be obtained from Eq. (2.41) by setting $e_{33} = 0$. Since for the plane stress case σ_{33} is identically zero, the corresponding strain component e_{33} can be evaluated from Eq. (2.39) as

$$e_{33} = (D_I - J_I)(\sigma_{11} + \sigma_{22}) + H_{33}.$$

Note that the use of creep and shear compliances as material property input allows the Poisson's ratio to be time-dependent. Hence, the

prsent formulation is applicable to any thermorheologically simple isotropic viscoelastic material over any length of time.

For the special case where the Poisson's ratio is a constant with time, then

$$J(\psi) = (1 + \nu)D(\psi). \tag{2.42}$$

The matrix [N] takes the form,

$$[N] = D_I \begin{bmatrix} 1 & -\nu & 0 & -\nu \\ -\nu & 1 & 0 & -\nu \\ 0 & 0 & 2(1+\nu) & 0 \\ -\nu & -\nu & 0 & 1 \end{bmatrix}$$

and, the corresponding hereditary strains are,

$$H_{11} = Q_{11} - \nu(Q_{22} + Q_{33})$$

$$H_{22} = Q_{22} - \nu(Q_{11} + Q_{33})$$

$$H_{12} = 2(1 + \nu)Q_{12}$$

$$H_{33} = Q_{33} - \nu(Q_{11} + Q_{22}) \tag{2.43}$$

If the viscoelastic properties of a material are defined by its bulk and shear compliances instead of the creep and shear compliances, then the creep compliance $D(\psi)$ in Eq. (2.27) is replaced by the bulk and shear properties. Using the viscoelastic relationship betwen creep, bulk and shear compliances given by,

$$D(\psi) = \frac{1}{9} M(\psi) + \frac{2}{3} J(\psi), \tag{2.44}$$

and substituting in Eq. (2.27), the relation in Eq. (2.39) is obtained. However, for this case the matrix [N] has the form,

$$[N] = \begin{bmatrix} (\frac{1}{9} M_I + \frac{2}{3} J_I) & (\frac{1}{9} M_I - \frac{1}{3} J_I) & 0 & (\frac{1}{9} M_I - \frac{1}{3} J_I) \\ (\frac{1}{9} M_I - \frac{1}{3} J_I) & (\frac{1}{9} M_I + \frac{2}{3} J_I) & 0 & (\frac{1}{9} M_I - \frac{1}{3} J_I) \\ 0 & 0 & 2J_I & 0 \\ (\frac{1}{9} M_I - \frac{1}{3} J_I) & (\frac{1}{9} M_I - \frac{1}{3} J_I) & 0 & (\frac{1}{9} M_I + \frac{2}{3} J_I) \end{bmatrix} \tag{2.45}$$

and the corresponding hereditary strains are,

$$H_{11} = \frac{1}{9} (Q_{11} + Q_{22} + Q_{33}) + \frac{2}{3} P_{11} - \frac{1}{3} (P_{22} + P_{33})$$

$$H_{22} = \frac{1}{9} (Q_{11} + Q_{22} + Q_{33}) + \frac{2}{3} P_{22} - \frac{1}{3} (P_{11} + P_{33})$$

$$H_{12} = 2P_{12}$$

$$H_{33} = \frac{1}{9} (Q_{11} + Q_{22} + Q_{33}) + \frac{2}{3} P_{33} - \frac{1}{3} (P_{11} + P_{22}) . \tag{2.46}$$

2.4 Finite Element Model

This section describes the finite element implementation of the nonlinear viscoelastic constitutive law presented in Sections 2.2 and 2.3. Since viscoelastic materials often undergo large displacements especially when subjected to creep type of loading, the geometrically nonlinear analysis described in [1,2] has been incorporated into the viscoelastic formulation.

Invoking the principle of virtual work and following the procedure outlined in [1,2], one has

$$\int_{V_1} {}_1M_{ijrs}\, {}_1e_{rs}\delta({}_1e_{ij})dV + \int_{V_1} {}_1\tau_{ij}\delta({}_1\eta_{ij})dV$$

$$= -\int_{V_1} {}_1\tau_{ij}\delta({}_1e_{ij})dV + \int_{V_1} {}_1f_i\delta u_i dV + \int_{S_1} {}_1t_i\delta u_i dS, \qquad (2.47)$$

where, ${}_1M_{ijrs}$ are the components of the viscoelasticity constitutive tensor. The rest of the quantities and the superscripts in Eq. (2.47) have the same definitions as given in [2]. Let each displacement increment at any time t be approximated as,

$$\Delta u_i = \sum_{j=1}^{n} \Delta u_i^j \psi_j(x_1, x_2). \qquad (2.48)$$

Substitution of Eq. (2.48) into Eq. (2.47) gives

$$([K^L] + [K^\sigma])\{\Delta u\} = \{F^L\} - \{F^\sigma\}, \qquad (2.49)$$

where

$$[K^L] = h\int_{A_1} [B^L]^T[M][B^L]dA, \quad h = \text{thickness} \qquad (2.50)$$

and [M] is the 4x4 viscoelastic constitutive matrix defined in Eq. (2.41). Note that for the nonlinear viscoelastic case, the 'linear' stiffness matrix $[K^L]$ is not really linear, but has nonlinearities imbedded in it due to the presence of the material kernel functions (g_0, g_1, g_2) in the matrix [M]. The nonlinear stiffness matrix $[K^\sigma]$ is the direct result of the geometrically nonlinear formulation and is given by

$$[K^\sigma] = h\int_{A_1} [B^\sigma]^T[\tau][B^\sigma]dA. \qquad (2.51)$$

The definitions of matrices $[B^L]$, $[B^\sigma]$, $\{F^L\}$, $\{F^\sigma\}$ and $[\tau]$ are the same as in [2]. The Cauchy stress components are computed by using the viscoelastic relation,

$$\{\sigma\} = [M](\{e\} - \{H\}) \qquad (2.52)$$

which has been derived in Section 2.3. For a geometrically nonlinear

analysis, the vector $\{e\}$ contains components of the Almansi strain tensor

$$e_{km} = \frac{1}{2}\left(\frac{\partial u_k}{\partial x_m} + \frac{\partial u_m}{\partial x_k} - \frac{\partial u_n}{\partial x_k}\frac{\partial u_n}{\partial x_m}\right) - \delta_{km}\theta \,. \tag{2.53}$$

It is evident that Eq. (2.49) contains two possible sources of nonlinearities: material nonlinearity due to Schapery's law and, geometric nonlinearity arising from the large displacement (and small strain) formulation. In order to obtain a solution to this nonlinear equation at any time step, the Newton-Raphson iterative technique is used. The incremental displacement $\{\Delta u\}_r$ obtained at the end of the r^{th} iteration is used to update the total displacement for the n^{th} time step,

$$^{n}u_r = {}^{n}u_{r-1} + \Delta^{n}u_r \tag{2.54}$$

The iterative procedure continues until a convergence criterion is satisfied. After that, the solution proceeds to the next time step. Note that for the first time-step, the initial condition $^{n}u_{r-1} = 0$ is used.

3. MOISTURE DIFFUSION AND DELAYED FAILURE

3.1 Governing Equations for Diffusion

The nonlinear Fickean two-dimensional, diffusion model presented in the present study is the one investigated by Lefebvre, et al. [12]. The diffusion model can also be applied for penetrants other than moisture, as long as the diffusion process is Fickean.

Fick's law for the two-dimensional diffusion of a penetrant within an isotropic material is given by

$$\frac{\partial}{\partial x}\left(D\,\frac{\partial C}{\partial x}\right) + \frac{\partial}{\partial y}\left(D\,\frac{\partial C}{\partial y}\right) = \frac{\partial C}{\partial t}, \qquad (3.1)$$

where, c is the penetrant concentration, which is a function of position and time, and D is the diffusion coefficient.

In order to model the transport phenomena in polymeric materials, Lefebvre et al. [12] derived a nonlinear diffusion coefficient based on the concept of free volume. According to this theory, the diffusion coefficient for a polymeric material above its glass transition temperature is given by,

$$D = \frac{D_o}{T_o} T e^{-B\{1/f - 1/f_o\}}, \qquad (3.2)$$

where D is the diffusion coefficient, T is the temperature, f is the free volume fraction, and B is a material constant. The subscript 'o' denotes values at the reference state. It is then postulated that the change in fractional free volume is due to changes in temperature, penetrant concentration, and the transient component of the mechanically induced dilatational strain. It is further assumed that these changes are additive, which is similar to the assumptions made by Knauss and Emri [15]. Thus

$$f = f_o + 3\alpha\Delta T + \Delta e_{kk} + 3\gamma c^N. \qquad (3.3)$$

In Eq. (3.3), α is the linear coefficient of thermal expansion, γ is the linear coefficient of expansion due to moisture, N is an exponent for the saturated state, and Δe_{kk} is the transient component of the mechanically induced dilatational strain. The dilatational strain due to the ambient stress state can be written as

$$e_{kk} = e_{kk}(0) + \Delta e_{kk}, \qquad (3.4)$$

where $e_{kk}(0)$ and Δe_{kk} are the instantaneous and transient components of

the mechanically induced dilatational strain e_{kk}.

$$e_{kk}(0) = \frac{1}{3} M(0)\sigma_{kk} \tag{3.5}$$

$$\Delta e_{kk} = \frac{1}{3} \int_0^t M(\psi^t - \psi^\tau) \frac{\partial}{\partial \tau} (g_2 \sigma_{kk}) d\tau \tag{3.6}$$

where $M(\psi)$ is the bulk compliance of the material. Combining Eqs. (3.4) and (3.5), we obtain

$$\Delta e_{kk} = e_{kk} - \frac{1}{3} M(0)\sigma_{kk}. \tag{3.7}$$

Substitution of Eq. (3.7) into Eq. (3.3) and the result into Eq. (3.2) yields

$$D = \frac{D_o}{T_o} T \exp \left\{ \frac{B}{f_o} \left[\frac{3(\alpha \Delta T + \gamma c^N) + (e_{kk} - \frac{1}{3} M_o \sigma_{kk})}{f_o + 3(\alpha \Delta T + \gamma c^N) + (e_{kk} - \frac{1}{3} M_o \sigma_{kk})} \right] \right\}. \tag{3.8}$$

From the viscoelastic formulation presented in Section 2, it is evident that the dilatational strain e_{kk} is dependent on the stress history, temperature and penetrant concentration,

$$e_{kk} = e_{kk}(\sigma_{kk}, T, c) \tag{3.9}$$

Hence, the two sources of nonlinearity in Eq. (3.1) are moisture concentration c and dilatational strain e_{kk}. Consequently, in order to accurately model the penetrant transport phenomena, the diffusion boundary-value problem needs to be solved in conjunction with the nonlinear viscoelasticity boundary-value problem by using an iterative procedure. The same solution procedure can also be applied for diffusion in polymeric materials where the plasticizing effect of the penetrant may cause the viscoelastic time-scale shift factor to be concentration dependent,

$$a^t_{\sigma TC} = a(\sigma, T, c) \tag{3.10}$$

One example of such a shift factor definition can be found in the work of Knauss and Emri [15], where the authors have used the concept of free volume to define a shift factor

$$a(T,c,e_{kk}) = \exp\{-\frac{B}{f_o}\left(\frac{\alpha\Delta T + \gamma c + \lambda e_{kk}}{f_o + \alpha\Delta T + \gamma c + \delta e_{kk}}\right)\}, \qquad (3.11)$$

where λ is the coefficient of the dilatation term. Note that the coefficients α and γ in Eqs. (3.8) and (3.11) are, in general, functions of T, c and e_{kk} but have been assumed to be constant for the sake of simplicity. This assumption is valid for temperatures above the glass transition temperature and below the boiling point of the penetrant.

3.2 Finite Element Formulation

Fick's law for two dimensional diffusion in a homogeneous isotropic material is given by,

$$\frac{\partial}{\partial x}\left(D\frac{\partial c}{\partial x}\right) + \frac{\partial}{\partial y}\left(\frac{\partial c}{\partial y}\right) = \frac{\partial c}{\partial t} \quad \text{in } \Omega \qquad (3.12)$$

subject to the boundary conditions,

$$D\frac{\partial c}{\partial x}n_x + D\frac{\partial c}{\partial y}n_y + \hat{q} = 0 \text{ on } \Gamma_1 \quad , \quad t \geq 0 \qquad (3.13)$$

$$c = \hat{c} \text{ on } \Gamma_2 \quad , \quad t \geq 0 \qquad (3.14)$$

and the initial condition,

$$c = c_o \text{ in } \Omega \quad , \quad t = 0 \qquad (3.15)$$

where, Ω is the two-dimensional region in which diffusion occurs, and Γ is the boundary of Ω.

The finite-element formulation of Eqs. (3.12)-(3.15) can be developed following the variational procedure used by Reddy [17]. The time dependent moisture concentration is approximated over an element

Ω^e as,

$$c^e(x,y,t) = \sum_{j=1}^{N} \psi_j^e(x,y) c_j^e(t) \tag{3.16}$$

where N is the number of nodes per element. The resulting finite-element equations cast in a matrix form are given by

$$[M^{(e)}]\{\dot{c}\} + [K^{(e)}]\{c\} = \{F^{(e)}\} \tag{3.17}$$

where

$$M_{ij}^{(e)} = \int_{\Omega^e} \psi_i^e \psi_j^e dxdy \tag{3.18a}$$

$$K_{ij}^{(e)} = \int_{\Omega^e} D\left(\frac{\partial \psi_i^e}{\partial x}\frac{\partial \psi_j^e}{\partial x} + \frac{\partial \psi_i^e}{\partial y}\frac{\partial \psi_j^e}{\partial y}\right)dxdy \tag{3.18b}$$

$$F_i^{(e)} = -\int_{\Gamma^e} \psi_i^e \hat{q} ds . \tag{3.19}$$

The time derivative $\{\dot{c}\}$ is approximated using the θ-family of approximation,

$$\theta\{\dot{c}\}_{n+1} + (1-\theta)\{\dot{c}\}_n = \frac{\{c\}_{n+1} - \{c\}_n}{\Delta t_{n+1}} \quad \text{for } 0 \le \theta \le 1 \tag{3.20}$$

where Δt_n is the time step and $\{c\}_n$ denotes the value of $\{c\}$ at time t_n. Using the approximations (3.22) in (3.18) for time t_n and t_{n+1} gives

$$[A^{(e)}]\{c\}_{n+1} - [B^{(e)}]\{c\}_n - \{P^{(e)}\}_n = 0 \tag{3.21}$$

where

$$[A^{(e)}] = [M^{(e)}] + \theta\Delta t_{n+1}[K^{(e)}]$$

$$[B^{(e)}] = [M^{(e)}] - (1-\theta)\Delta t_{n+1}[K^{(e)}]$$

$$\{P^{(e)}\} = \Delta t_{n+1}(\theta\{F^{(e)}\}_{n+1} + (1-\theta)\{F^{(e)}\}_n). \tag{3.22}$$

Recognizing that a source of nonlinearity in the form of the diffusion coefficient D is imbedded in the matrix $[K^{(e)}]$, the Newton-Raphson technique is employed to solve for the concentration $\{c\}_{n+1}$ at each time step. Note that for n = 0, the vector $\{c\}_0$ in Eq. (3.21) is known from the initial conditions.

3.3 Delayed Failure: Uniaxial Formulation

When a viscoelastic material undergoes deformation, only a part of the total deformation energy is stored, while the rest of the energy is dissipated. This behavior is unlike elastic material where all the energy of deformation is stored as strain energy. Reiner and Weisenberg [5] postulated that it is this time-dependent energy storage capacity that is responsible for the transition from viscoelastic response to yield in ductile materials or fracture in brittle ones. According to this theory, failure occurs when the stored deviatoric strain energy per unit volume in a body reaches a certain maximum value called the resilience, which is a material property. Note that when there is no dissipation, that is, when the material is elastic, then Reiner-Weisenberg criterion becomes identical to the von Mises criterion.

Consider the single Kelvin element shown in Fig. 1, subject to the uniaxial tensile load $\sigma(t)$. The total strain response e(t) due to the applied stress can be divided into two components: the instantaneous respone e_0, and the transient response $e_1(t)$,

$$e(t) = e_0 + e_1(t) \tag{3.23}$$

For uniaxial creep, the applied stress $\sigma(t)$ is given as

$$\sigma(t) = \sigma_0 H(t) \tag{3.24}$$

where H(t) is the unit step function.

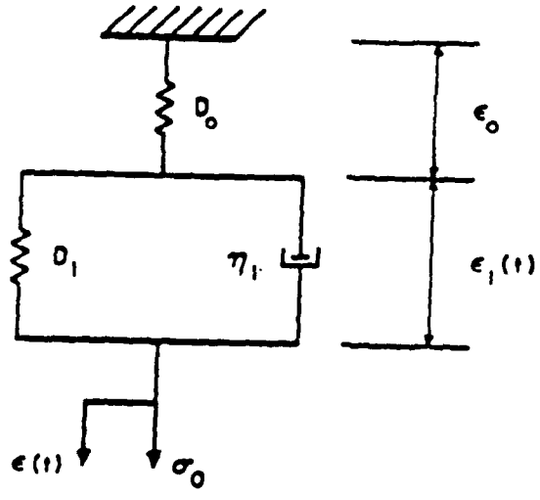

Figure ' A Single Kelvin Unit Subject to Uniaxial Stress.

Substituting Eq. (3.24) into Schapery's nonlinear uniaxial single integral law given by Eq.(2.1) and expressing the transient creep compliance $D_c(\psi)$ as

$$D_c(\psi) = D_o - D_1(1 - e^{-\lambda_1\psi}) \tag{3.25}$$

leads to,

$$e(\psi) = g_o D_o \sigma_o + g_1 g_2 \sigma_o D_1 (1 - e^{-\lambda_1\psi}) \tag{3.26}$$

where ψ is the reduced time defined in Eq. (2.2).

Comparing Eq. (3.26) with (3.23), it follows that

$$e_o = g_o D_o \sigma_o$$

$$e_1(\psi) = g_1 D_1 (1 - e^{-\lambda_1\psi}) g_2 \sigma_o . \tag{3.27}$$

For a given applied stress σ_o, the stress developed in the nonlinear spring with compliance $D_o g_o$ is σ_o^s and the corresponding strain is e_o^s. For the spring with the nonlinear compliance $D_1 g_1$ the stress is given by,

$$\sigma_1^s = \frac{e_1^s}{g_1 D_1} \tag{3.28}$$

where the superscript 's' denotes quantities related to the spring. From Fig. 1 it is evident that e_1^s and e_1 are equivalent. Hence,

$$\sigma_1^s = g_2(1 - e^{-\lambda_1\psi})\sigma_o . \tag{3.29}$$

The total energy, W^s, stored in the two springs over time t is (see Hiel et al. [14]),

$$W^s = \int_0^{e_o} \sigma_o^s de + \int_0^t \sigma_1^s \dot{e}_1^s dt$$

$$= \frac{1}{2} g_o D_o \sigma_o^2 + \frac{1}{2} g_1 D_1 [1 - e^{-\lambda_1\psi}]^2 (g_2\sigma_o)^2 . \tag{3.30}$$

For a viscoelastic material represented by multiple Kelvin elements in series, Eq. (3.30) takes the form,

$$W^S = \frac{1}{2} g_o D_o \sigma_o^2 + \frac{1}{2} g_1 g_2^2 \sigma_o^2 \sum_{r=1}^{n} [D_r(1 - e^{-\lambda_r \psi})^2]. \qquad (3.31)$$

According to the Reiner-Weisenberg hypothesis, failure occurs when the stored energy W^S reaches the resilience of the material. Denoting the resilience as R, the expression for the time dependent failure stress obtained from Eq. (3.31) for uniaxial stress state is,

$$\sigma_f = \frac{\sqrt{R}}{\left\{\frac{1}{2} g_o D_o + \frac{1}{2} g_1 g_2^2 \sum_{r=1}^{n} [D_r(1 - e^{-\lambda_r \lambda})^2]\right\}^{1/2}}. \qquad (3.32)$$

3.4 Delayed Failure: Multiaxial Formulation

If σ_1, σ_2 and σ_3 are the principal stresses at any point in a viscoelastic material, then by definition, the shear stresses are zero on the principal planes. In order to simplify the derivation, let it be assumed that the viscoelastic material is represented by means of a single Kelvin element (see Fig. 1) in each principal direction. The applied multiaxial creep stresses in the material principal directions are given by,

$$\begin{aligned} \sigma_{11} &= \sigma_1 H(t) \\ \sigma_{22} &= \sigma_2 H(t) \\ \sigma_{33} &= \sigma_3 H(t). \end{aligned} \qquad (3.33)$$

Substitution of Eqs. (3.33) in Eqs. (2.31) and (2.32) results in the following expressions for the corresponding viscoelastic strains,

$$e_{11}(t) = D_o[\sigma_1 + (1 - \frac{J_o}{D_o})\sigma_2 + (1 - \frac{J_o}{D_o})\sigma_3] + D_1[(1 - e^{-\lambda_r \psi})g_2\sigma_1$$

$$+ \{(1 - e^{-\lambda_r \psi}) + \frac{J_1}{D_1}(1 - e^{-\lambda_r \psi})\}g_2\sigma_2 + \{(1 - e^{-\lambda_r \psi})$$

$$\sigma^s_{oj} = -\nu(\sigma_1 + \sigma_2 + \sigma_3) + (1 + \nu)\sigma_i\delta_{ij}$$

$$\sigma^s_{rj} = -\nu g_2(1 - e^{-\lambda r^\psi})(\sigma_1 + \sigma_2 + \sigma_3) + (1 + \nu)g_2(1 - e^{-\lambda r^\psi})\sigma_i\delta_{ij}. \tag{3.44}$$

4. NUMERICAL RESULTS

In this section results of a number of linear elastic, linear viscoelastic and nonlinear viscoelastic analyses are discussed in light of available experimental or analytical results. All results are obtained using NOVA on an IBM 3090 computer in double precision arithmatic.

4.1 Elastic Analysis of a Composite Single Lap Joint

Renton and Vinson [18] used a closed form elastic solution to conduct a parametric study of the effect of adherend properties on the peak stresses within the adhesive in a composite single lap joint. A similar parametric study was carried out using the finite element program NOVA. The geometry, finite element discretization and boundary conditions for the composite lap joint are shown in Fig. 2. For the sake of simplicity, only identical adherends are considered. Each adherend is made up of seven laminas of equal thickness. The orthotropic material properties for a lamina are given in Table 1. In order to maintain material symmetry about the laminate mid-plane and thus eliminate bending-stretching coupling, a $\theta^\circ/0^\circ/-\theta^\circ/0^\circ/-\theta^\circ/0^\circ/\theta^\circ$ ply orientation was selected for the analysis. Note that this type of ply orientation places the θ° ply immediately adjacent to the adhesive layer. The adhesive used is FM-73 and its isotropic linear elastic properties are listed in Table 2. The adhesive layer is modeled using

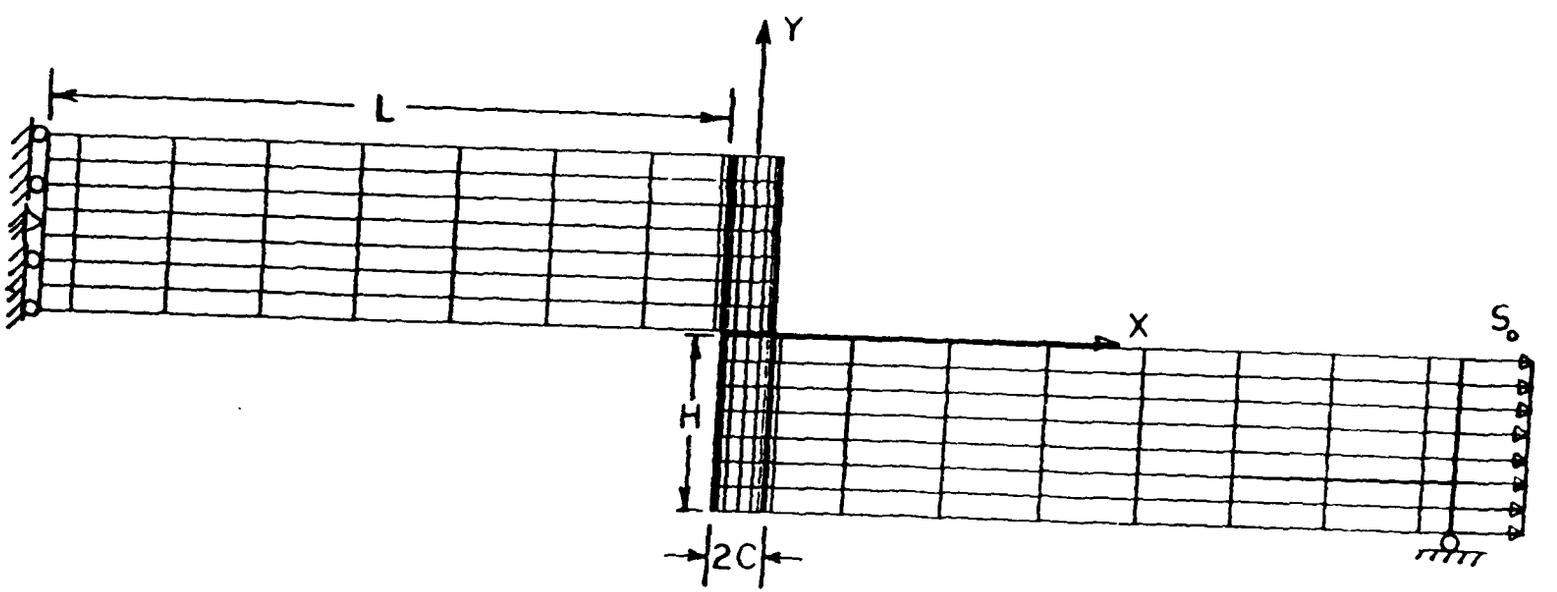

Figure 2. Specimen Geometry, Boundary Condition, and Finite Element Discretization for a Single Lap Joint with Composite Adherends (L = 107.0, H = 1.61, C = 4.0, Thickness of Adhesive Layer = 0.05, all dimensions in mm., Applied Stress = 2763 MPa.).

Table 1. Orthotropic Material Properites for Composite Adherend.

$$Q_{11} = 46.885 \times 10^3 \text{ MPa}$$

$$Q_{12} = Q_{13} = 4.137 \times 10^3 \text{ MPa}$$

$$Q_{22} = Q_{33} = 14.962 \times 10^3 \text{ MPa}$$

$$Q_{23} = Q_{32} = 2.068 \times 10^3 \text{ MPa}$$

$$Q_{44} = Q_{55} = Q_{66} = 3.447 \times 10^3 \text{ MPa}$$

Table 2. Isotropic Linear Elastic Properties for FM-73.

$E = 2.78 \times 10^3$ MPa

$G = 1.01 \times 10^3$ MPa

$\nu = 0.38$

sixteen eight-noded quadrilateral elements along its length and two elements through its thickness. A series of elastic finite element analyses is performed to study the effect of ply orientation, lamina primary modulus (Q_{11}), and geometric nonlinearity on the peak stresses in the adhesive.

In order to study the influence of ply orientation on the adhesive stress distribution, stress analyses were performed for $\theta = 0°$, $\theta = 15°$, $\theta = 45°$, and $\theta = 90°$ respectively. The results are shown in Figs. 3 and 4. The plots show the variation of stresses along the upper bondline of the overlap. The parameter x/c is the normalized distance from the bond centerline such that the value x/c = -1 corresponds to the left-hand free edge of the bond overlap. It is evident from these figures that an increase in the ply orientation angle θ, causes the peak stresses to increase near the free edge of the bond overlap. The adherend with a 0°/90° ply orientation (cross-ply) shows a 28% increase in peel stress and a 17% increase in shear stress over the corresponding values for a 0° (unidirectional) ply orientation. This is not surprising since a cross-ply adhererd has a lower bending stiffness which results in a larger lateral deflection causing higher stress concentrations at the overlap ends.

The influence of the lamina primary modulus (Q_{11}) on adhesive peel and shear stresses can be seen in Figs. 5 and 6 respectively. A unidirectional (0-degree) adherend ply orientation is used for this analysis. The two figures show a significant increase in the peak adhesive stress as the value of Q_{11} decreases. This is understandable as a more flexible adherend would undergo larger bending and hence produce higher stress concentrations at the overlap ends.

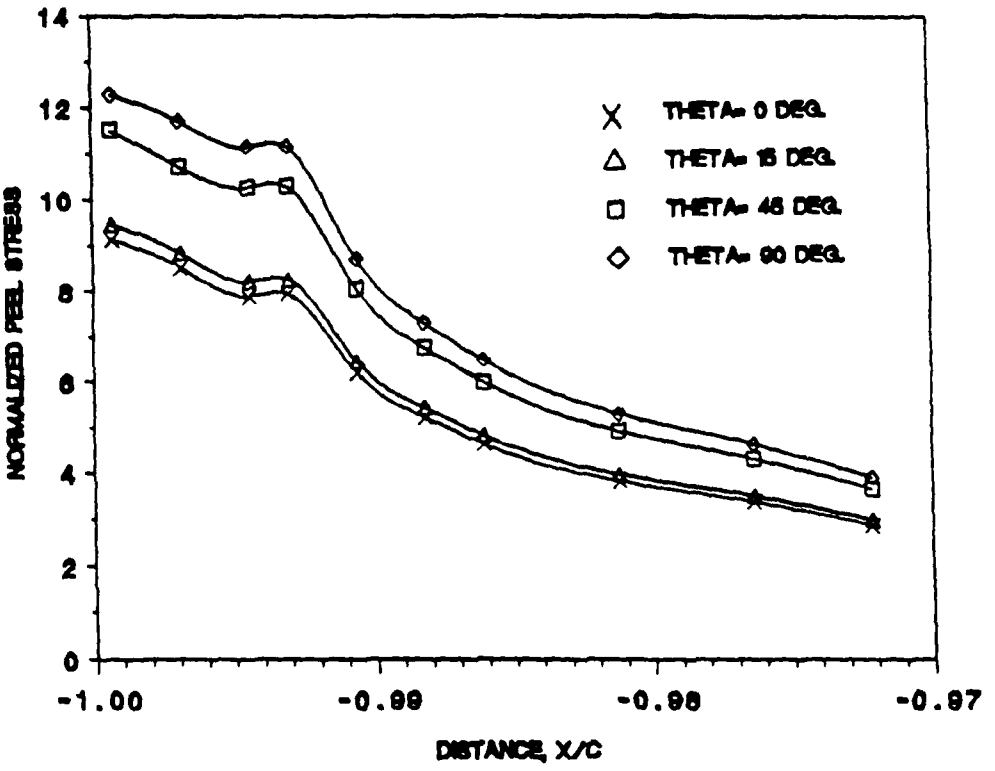

Figure 3 Influence of Ply Orientation on Adhesive Peel Stress.

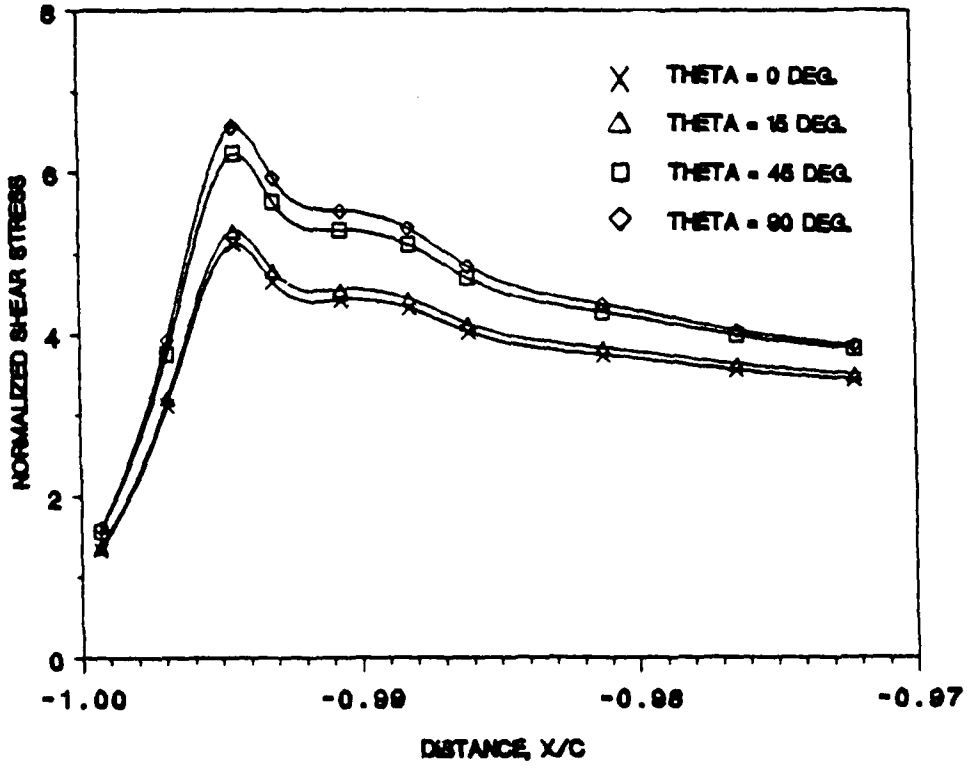

Figure 4 Influence of Ply Orientation on Adhesive Shear Stress.

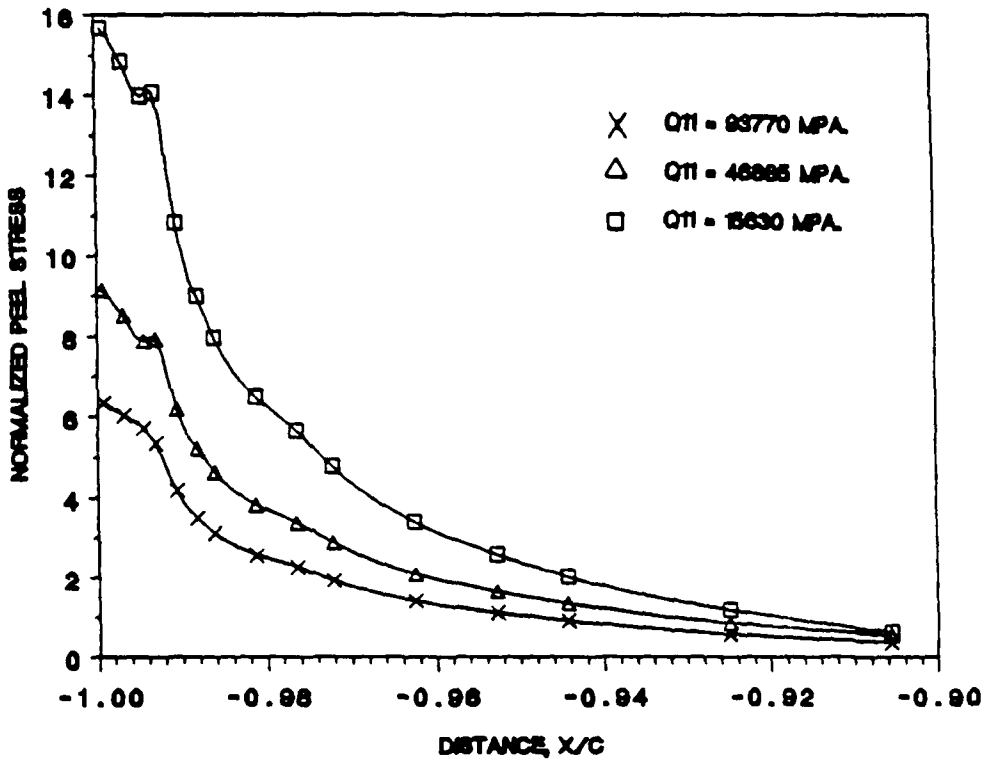

Figure 5 Influence of Q11 on Adhesive Peel Stress.

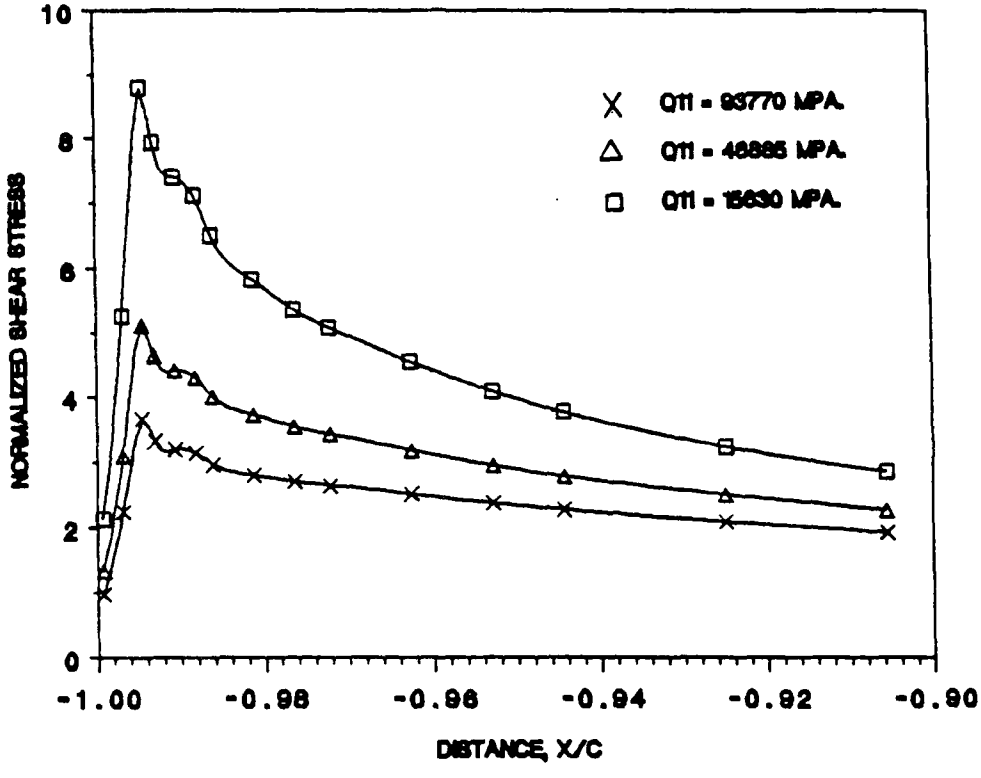

Figure 6 Influence of Q11 on Adhesive Shear Stress.

Harris and Adams [19] conducted large displacement finite element analyses on a single lap joint with aluminum adherends and observed significant reduction in peak stresses at the edge of the adhesive as compared to linear results. In order to observe the effect of geometric nonlinearity on a single lap joint with laminated composite adherends, a large displacement analysis was performed using the program NOVA. Due to its greater susceptibility to bending, cross-ply laminated adherends were used for this analysis. The results can be seen in Figs. 7 and 8. The geometrically nonlinear analysis results in a 30% reduction in the peak peel stress and a 15% reduction in the peak shear stress. The horizontal shifting of the nonlinear curves is due to the configuration coordinate update required by the large displacement analysis.

4.2 Nonlinear Viscoelastic Analysis of a Composite Single Lap Joint

A nonlinear viscoelastic analysis of a lap joint made of composite material was carried out over a time period of forty hours using NOVA. The specimen geometry and the finite element discretization are the same as for the elastic analysis as shown in Fig. 2. However, instead of a uniform end traction, a uniform end displacement of 0.363 mm is applied to the end of the joint and is held constant with time. The adherends are made of symmetric cross-ply laminates whose properties are given in Table 1, while the adhesive used is FM-73 and its creep compliance and Schapery parameters can be found in Table 3.

Figures 9 and 10 show the variation of shear stress and shear strain respectively across the entire bond length over a period of 40 hours. The sharp peak on the left-hand edge is due to the presence of a re-entrant corner and also due to the difference in material properties.

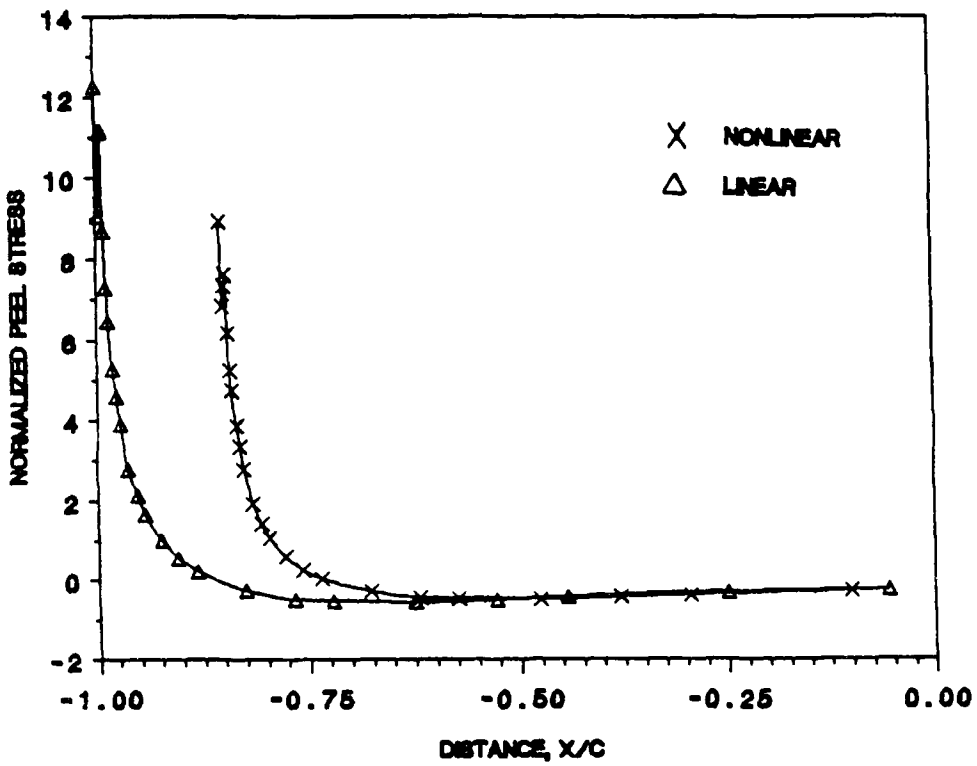

Figure 7. Influence of Geometric Nonlinearity on Adhesive Peel Stress.

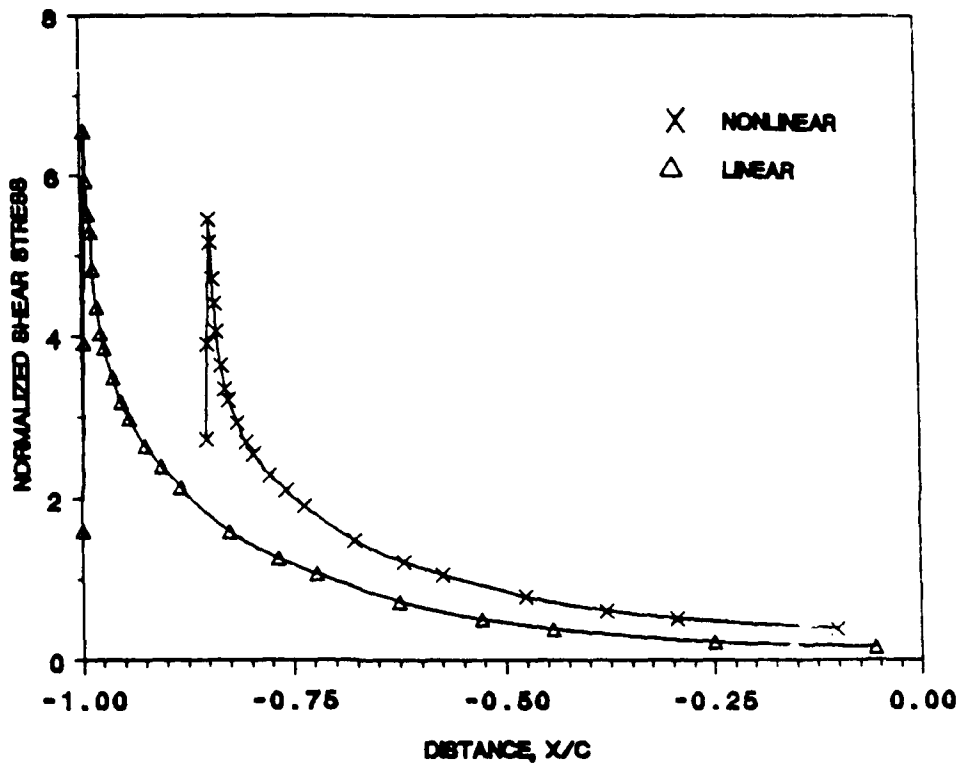

Figure 8. Influence of Geometric Nonlinearity on Adhesive Shear Stress.

Table 3. Material Data for FM-73 Unscrimmed at 30°C.

Elastic Compliance, D_o:	360×10^{-6}/MPa
Poisson's Ratio, ν:	0.38
Coefficient of Thermal Expansion, α:	6.6×10^{-5} m/m/°K

Prony Series Coefficients:

$D_1 = 11.05 \times 10^{-6}$/MPa	$\tau_1 = 10$ secs.
$D_2 = 12.27 \times 10^{-6}$/MPa	$\tau_2 = 10^2$ secs.
$D_3 = 17.35 \times 10^{-6}$/MPa	$\tau_3 = 10^3$ secs.
$D_4 = 21.63 \times 10^{-6}$/MPa	$\tau_4 = 10^4$ secs.
$D_5 = 13.13 \times 10^{-6}$/MPa	$\tau_5 = 10^5$ secs.
$D_6 = 41.78 \times 10^{-6}$/MPa	$\tau_6 = 10^6$ secs.

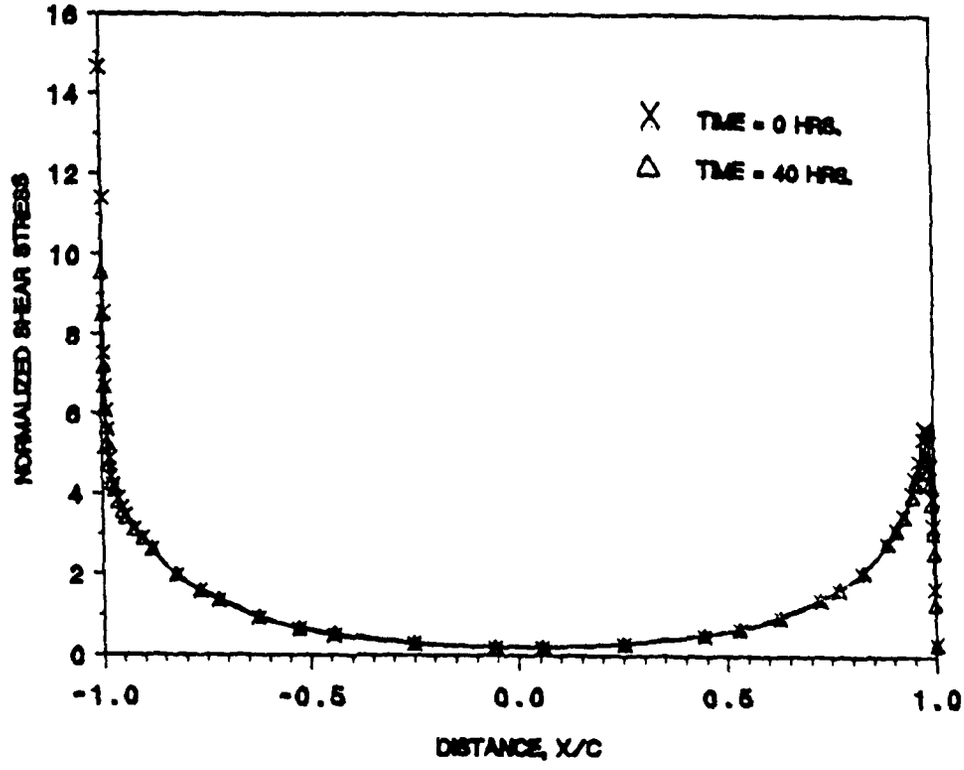

Figure 9 Variation of Shear Stress with Time for Entire Overlap.

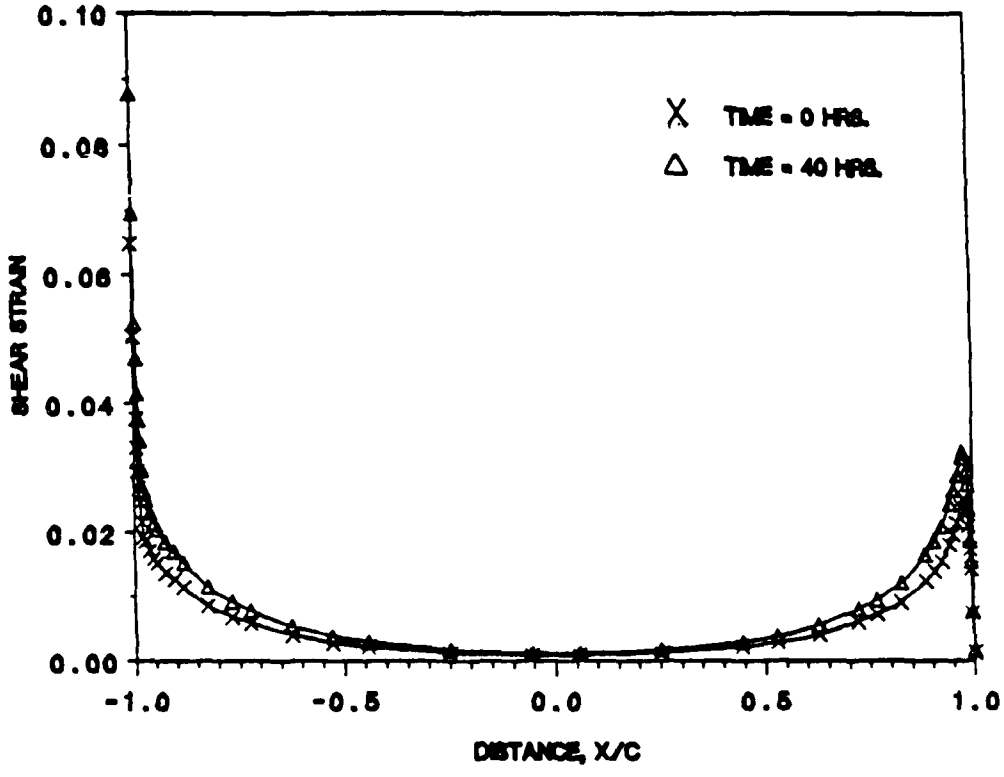

Figure 10 Variation of Shear Strain with Time for Entire Overlap.

Figures 11 and 12 provide a close-up view of the shear stress and strain gradients at the free edge. As might be expected, the shear stress undergoes relaxation which results in a 36% decrease in the peak value at the left hand edge. The stresses have been normalized with respect to an average shear stress value of 4.5 N/mm^2. The peak shear strain, however, shows an increase of 35% over the same period of time. Similarly, Figs. 13 to 16 reveal that while the peak values of the peel and axial stresses decrease by 26% and 32% respectively, the corresponding strains show a respective increase of 63% and 6%. The reason that the strains increase with time even though the joint end deflection remains fixed, is because the adherends are modeled as elastic continuums. As the stresses in the adhesive relax with time, the elastic adherends deform to attain a new equilibrium configuration and this leads to an altered state of strain within the adhesive. Hence, it is very important that the elastic nature of the adherends be taken into account in an analysis. Also, the significant increase in adhesive strains with time is a viscoelastic phenomenon and therefore it cannot be predicted by means of a purely elastic analysis. This fact emphasizes the need to model the adhesive layer as a viscoelastic medium in order to be able to predict the long-term durability of a bonded joint.

4.3 Nonlinear Fickean Diffusion in Polystyrene

In order to validate the diffusion model implemented in NOVA and discussed in Section 3, results from a nonlinear diffusion analysis presented in [20] are used. The test problem involves unsteady sorption of a penetrant in a semi-infinite medium for a diffusion coefficient that is an exponential function of penetrant concentration, that is,

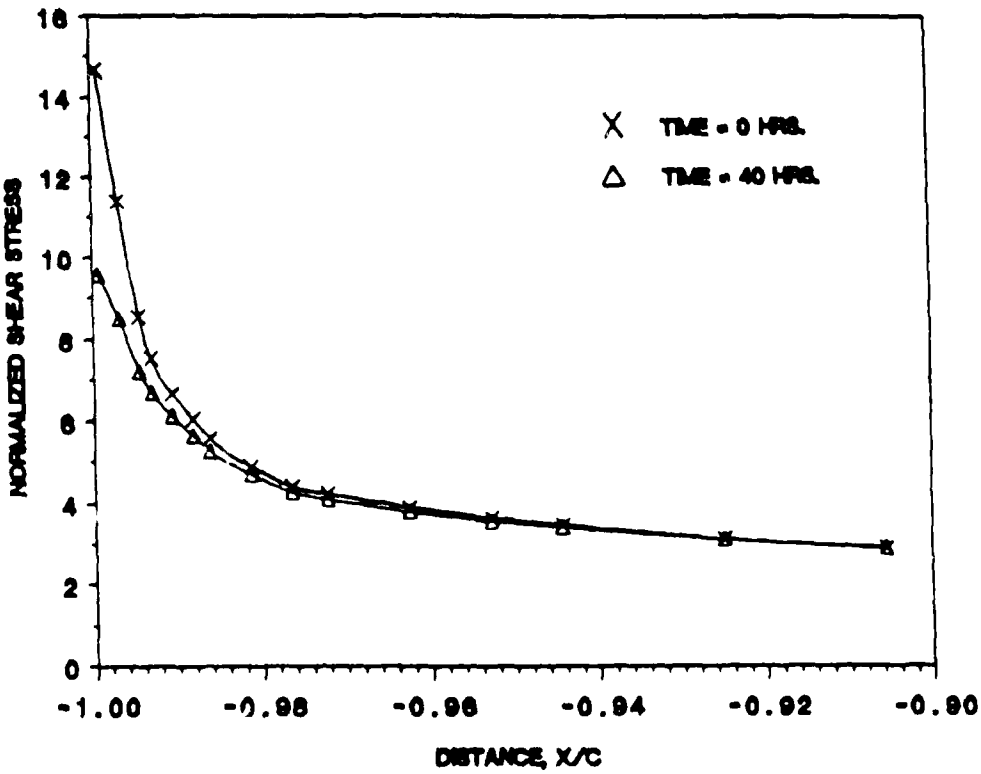

Figure 11 Variation of Shear Stress with Time Near the Free Edge.

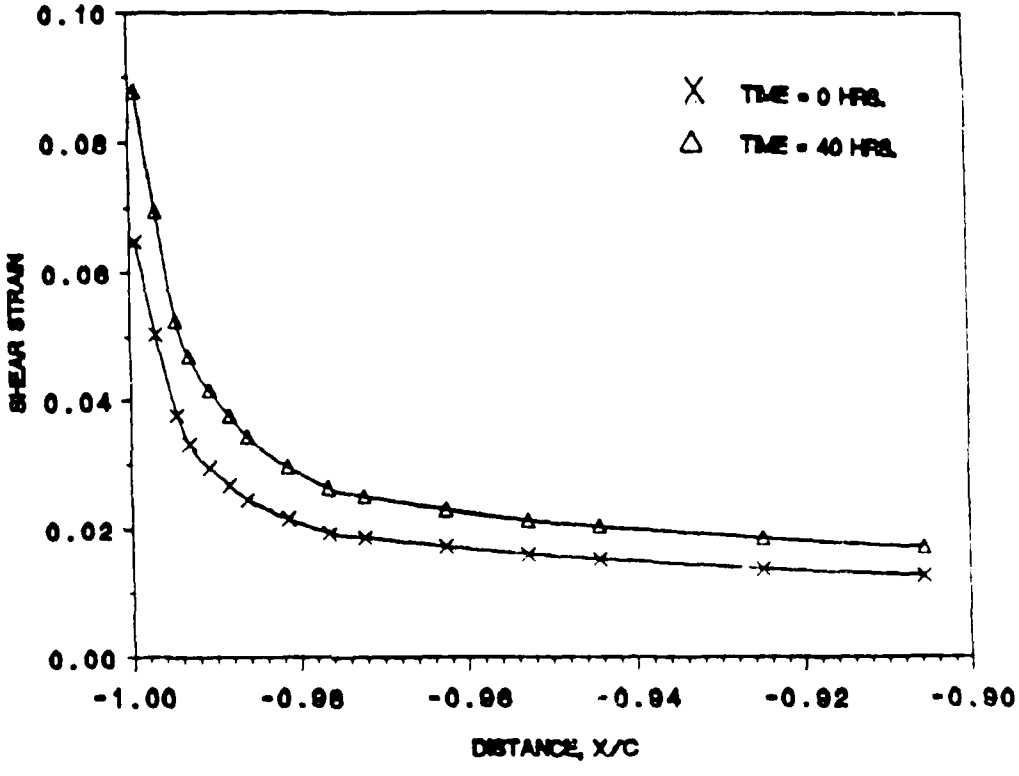

Figur. 12 Variation of Shear Strain with Time Near the Free Edge.

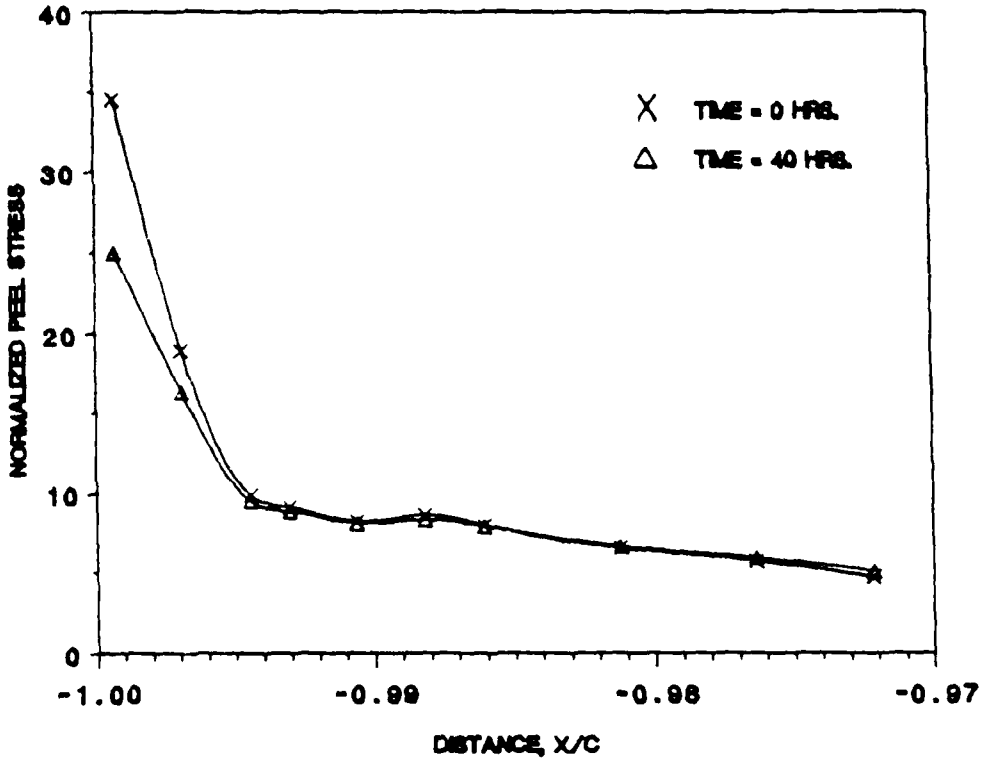

Figure 13 Variation of Peel Stress with Time Near the Free Edge.

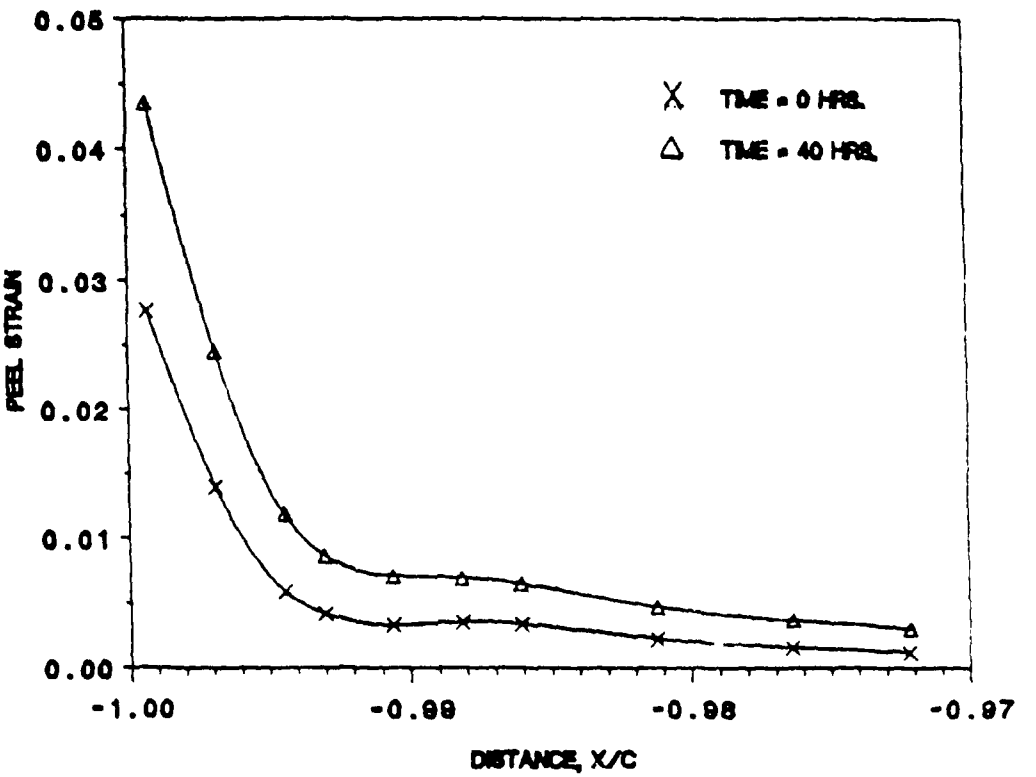

Figur 4 Variation of Peel Strain with Time Near the Free Edge.

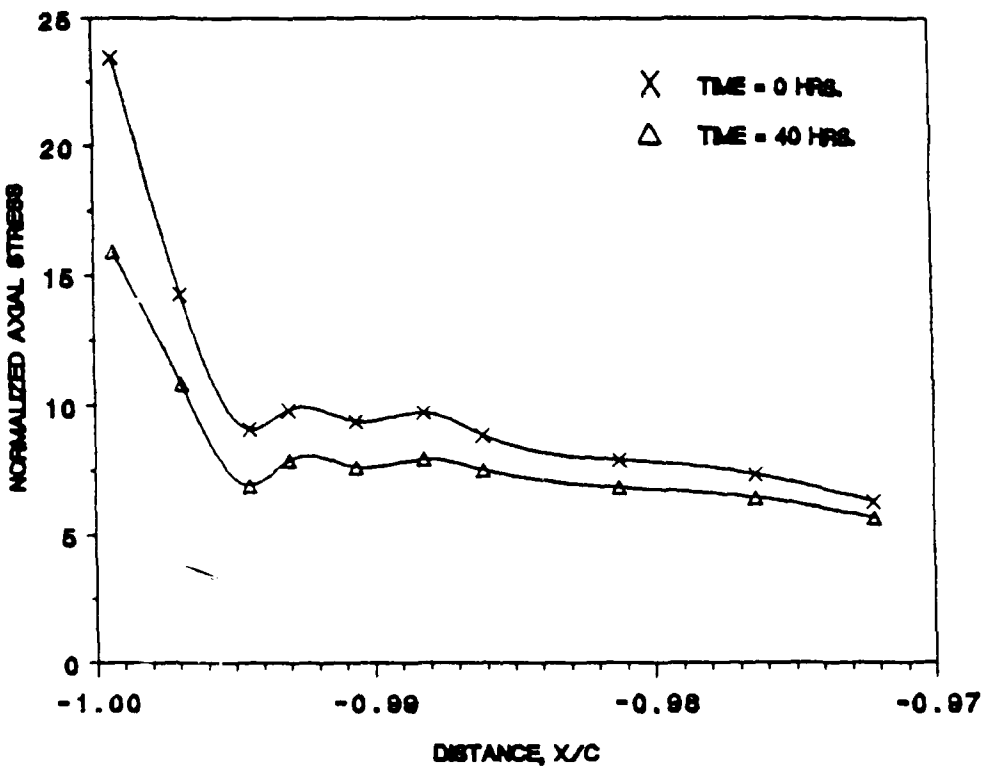

Figure 15 Variation of Axial Stress with Time Near the Free Edge.

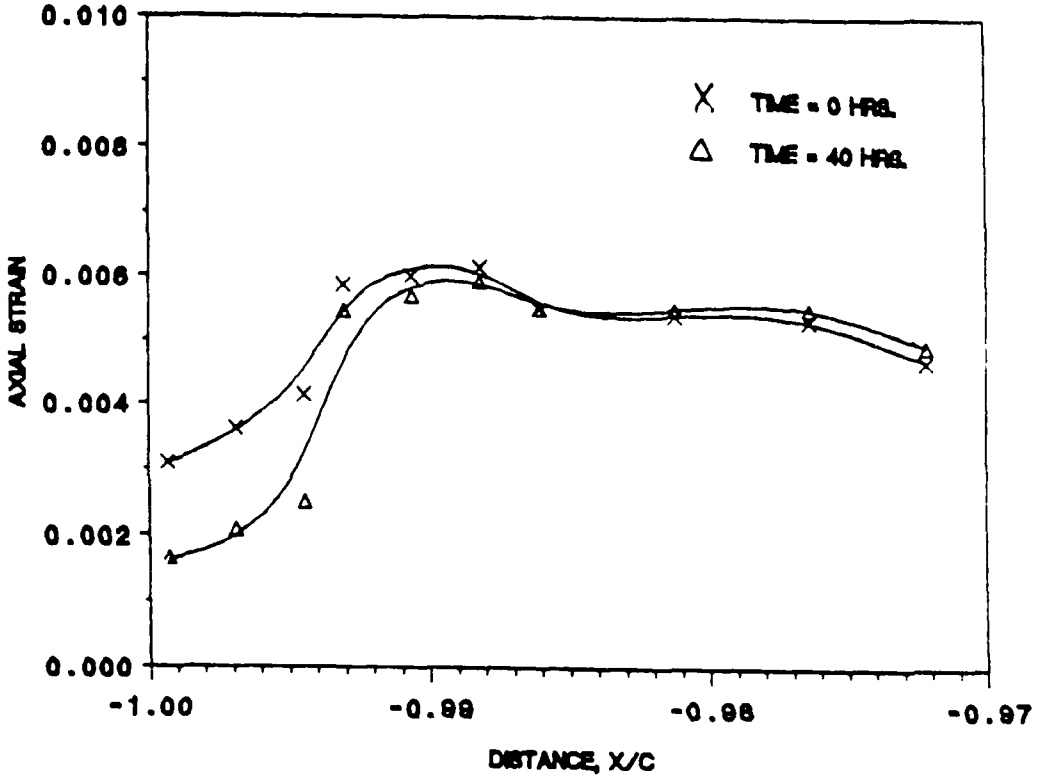

Figure 16 Variation of Axial Strain with Time Near the Free Edge.

$D = D_0 \exp(kC/C_0)$. Finite element predictions were obtained for k = 2.614 and k = 3.912 and the results were compared with the published results represented by the solid lines in Fig.17. Excellent agreement is observed for the two values of the coefficient k.

Levita and Smith [21] conducted experiments to study gas transport in polystyrene and found that the diffusion coefficients for gases decreased with time when the polystyrene film was subject to a constant uniaxial strain. This effect was attributed to the continuous free volume recovery (densification) in the polystyrene specimen at constant strain. The study also indicated that larger free volume elements increase in size faster than the smaller ones as volume recovery progresses. Using the results published in [21] as a guideline, NOVA was used to study the time dependence of the diffusion coefficient for carbon-dioxide gas in a polystyrene film at constant strain. For this case, the temprature and moisture concentration effects presented in Eq. (3.8) were neglected, resulting in a diffusion coefficient that is solely a function of the transient component of the dilatational strain which, in turn, is a measure of the change in the free volume. Figure 18 shows the variation of the diffusion coefficient with time for three different strain levels. The material properties for polystyrene which were obtained from [21] are given in Table 4. From Fig.18 it is evident that, independent of the strain level, the diffusion coefficient reaches a peak value at around t = 1 hour and then slowly decays to the reference value, D_0. This behavior can be attributed to an initial increase in free volume due to the application of the uniaxial strain, followed by a continuous recovery in free volume (densification) at a constant strain as the polystyrene film undergoes relaxation. A larger

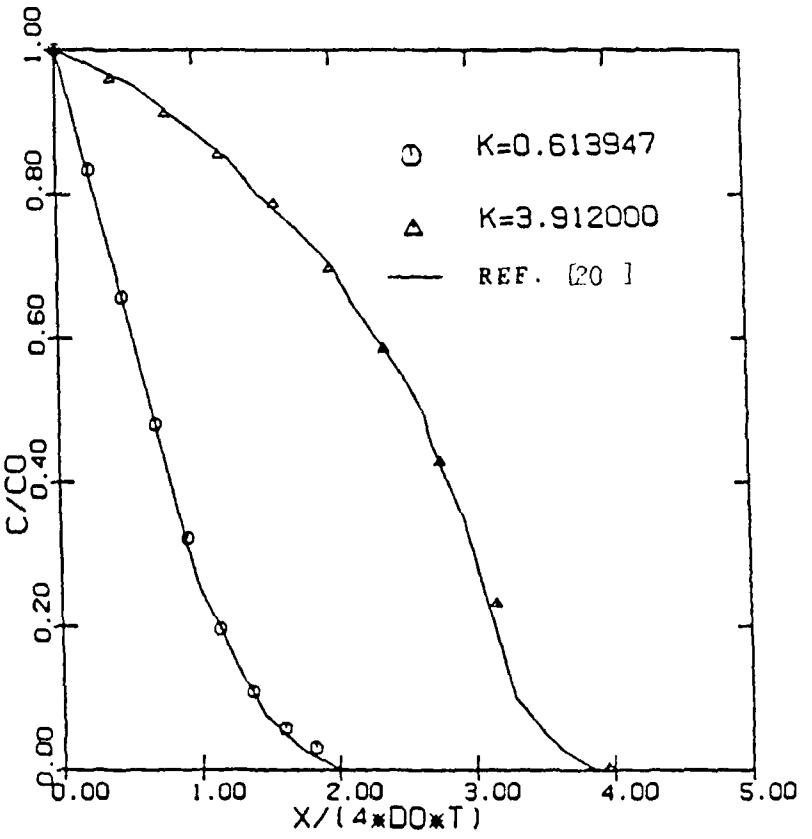

Figure 17 Profiles for the Unsteady Sorption of a Penetrant in a Semi-Infinite Medium.

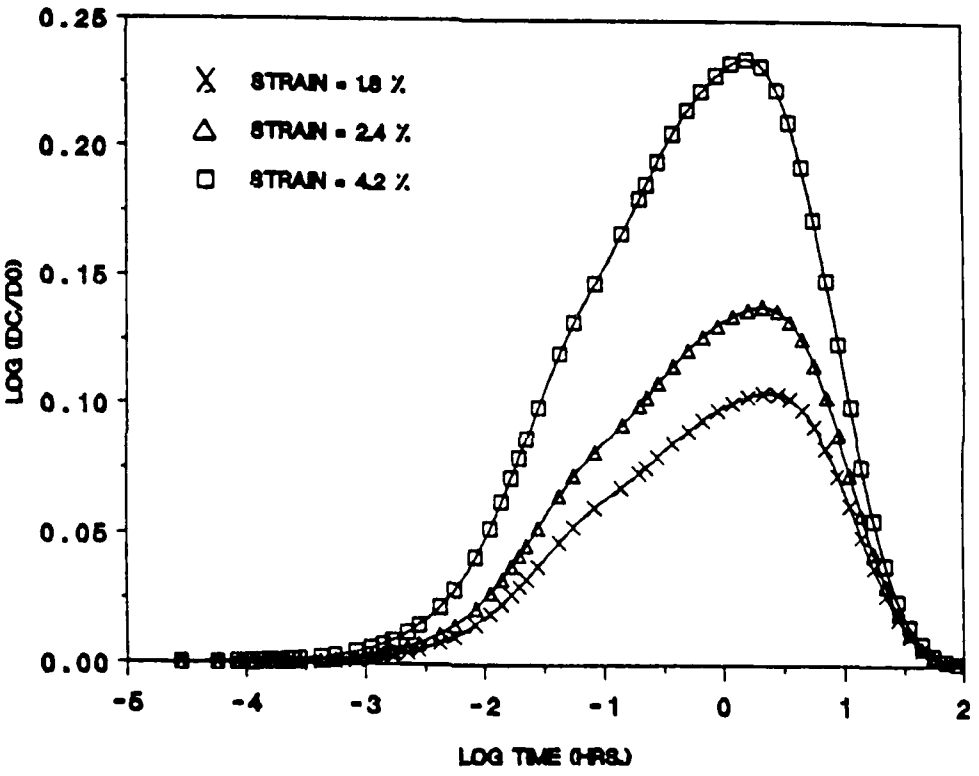

Figure 18 Effect of Mechanical Strain on the Diffusion Coefficient for Polystyrene.

Table 4. Material Properties for Polystyrene at 50 °C.

Bulk Compliance:

$M_0 = 1.2 \times 10^{-4}$/MPa	
$M_1 = 0.2896 \times 10^{-4}$/MPa	$\tau_1 = 1.515 \times 10^{2}$ sec.
$M_2 = 0.2246 \times 10^{-4}$/MPa	$\tau_2 = 1.515 \times 10^{3}$ sec.
$M_3 = 0.3721 \times 10^{-4}$/MPa	$\tau_3 = 1.515 \times 10^{4}$ sec.
$M_4 = 0.1354 \times 10^{-4}$/MPa	$\tau_4 = 1.515 \times 10^{5}$ sec.

Shear Compliance:

$J_0 = 1.0 \times 10^{-3}$/MPa	
$J_1 = 2.16$/MPa	$\tau_1 = 1.515 \times 10^{8}$ sec.
$J_2 = 2.92$/MPa	$\tau_2 = 1.515 \times 10^{10}$ sec.
$J_3 = 1.38$/MPa	$\tau_3 = 1.515 \times 10^{12}$ sec.
$J_4 = 2.88$/MPa	$\tau_4 = 1.515 \times 10^{13}$ sec.
$J_5 = 2.31$/MPa	$\tau_5 = 1.515 \times 10^{14}$ sec.
$J_6 = 3.59$/MPa	$\tau_6 = 1.515 \times 10^{15}$ sec.
$J_7 = 0.648$/MPa	$\tau_7 = 1.515 \times 10^{16}$ sec.

Reference free volume $f_0 = 0.033$

Diffusion coefficient $D_0 = 9 \times 10^{-6}$ mm^2/sec

applied strain produces larger initial dilatation, and this results in a higher peak in the diffusion coefficient. Figure 18 also reveals that the time rate of free volume recovery, and hence the time rate of decrease in the diffusion coefficient, is proportional to the applied strain level.

The influence of penetrant molecule size on the diffusion coefficient for gases in polystyrene was studied by varying the magnitude of the material parameter B in Eq. (3.8). The temperature and strain were held constant at 50°C and 1.8% respectively. The prediction obtained from NOVA are shown in Fig. 19 for two values of B. The faster rate of decrease in the diffusion coefficient for a higher value of B implies that the larger free-volume elements decrease in size faster than the smaller ones as volume recovery progresses. The NOVA predictions are qualitatively in good agreement with the results presented in [21].

When a polymeric material is in the rubbery state, equilibrium is reached very rapidly in response to variations in temperature, stress and penetrant conentration. By contrast, a material in the glassy state is not in thermodynamic equilibrium and the response of the free volume to changes in external conditions is delayed. This metastable state causes the free volume to slowly collapse with time until equilibrium is reached. This phenomenon is known as physical aging and causes relaxation processes to take place over a longer time. Struik [23] proposed that for a material in the glassy state, effective time λ is related to actual time t by,

$$\lambda = \int_0^t \left(\frac{t_e}{t_e + \xi}\right)^{\mu} \cdot d\xi \qquad (4.1)$$

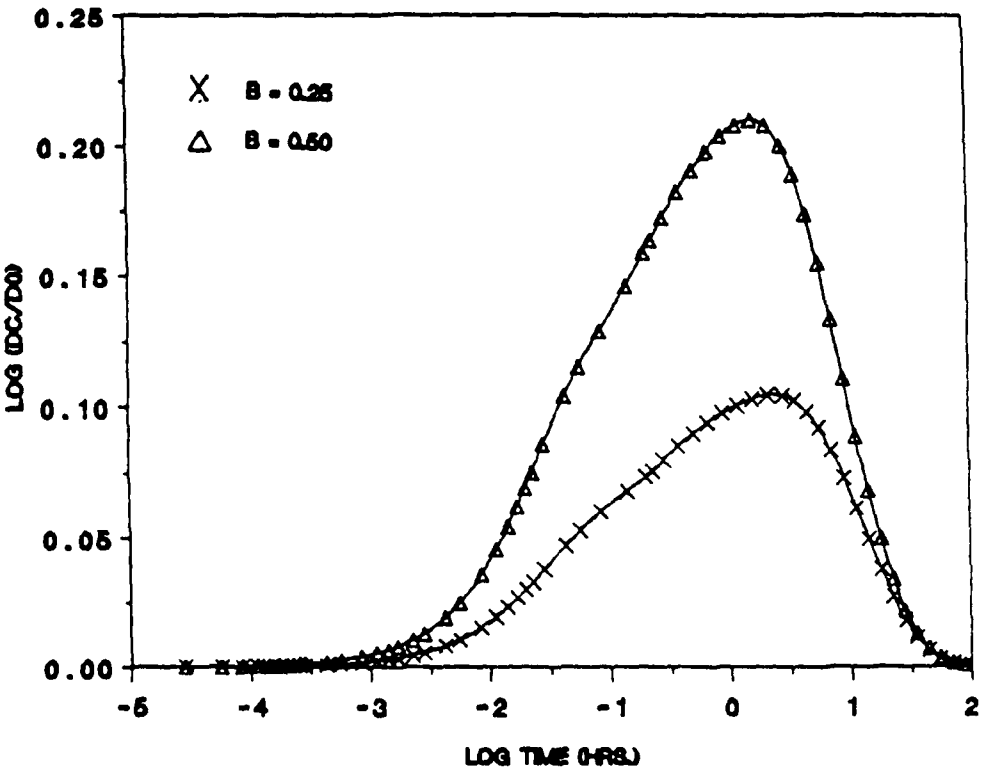

Figure 19 Effect of Material Parameter B on the Diffusion Coefficient for Polystyrene.

where t_e is the aging time at the start of service life or testing and μ is a constant such that $0 \leq \mu \leq 1$. For such a material, the definition of reduced time given by Eq. (2.2) is no longer valid and should be modified to,

$$\psi^{\lambda} = \int_0^{\lambda} (a^s_{\sigma T})^{-1} ds \qquad (4.2)$$

where $a^s_{\sigma T}$ is the shift factor.

The effect of physical aging on the diffusion coefficient for carbon-dioxide gas in polystyrene was studied by implementing Eqs. (4.1) and (4.2) in NOVA. The values of temperature, strain and t_e were set at 50°C, 1.8% and 24 hours respectively. Figure 20 shows that an increased physical aging denoted by a higher value of the parameter μ, causes the diffusion coefficient to decay slower than the one for which μ is lower. This behavior is expected since increased physical aging causes the free volume recovery to take place over a longer period of time. Note that when there is no physical aging, μ and t_e are equal to zero and λ is identically equal to t.

4.4 Nonlinear Viscoelastic Analysis of a Butt Joint Including Moisture Diffusion

The effect of a change in the free volume of a polymer on its viscoelastic response was discussed by Knauss and Emri [15]. They used the unifying concept of the free volume by considering that fractional free volume depends on three variables: temperature T, moisture concentration c, and mechanically induced dilatation θ. Lefevbre et al. [12] extended the free volume concept to define a nonlinear diffusion coefficient, which results in a coupling between the viscoelasticity and the diffusion boundary value problems (see Section 3.1). The influence

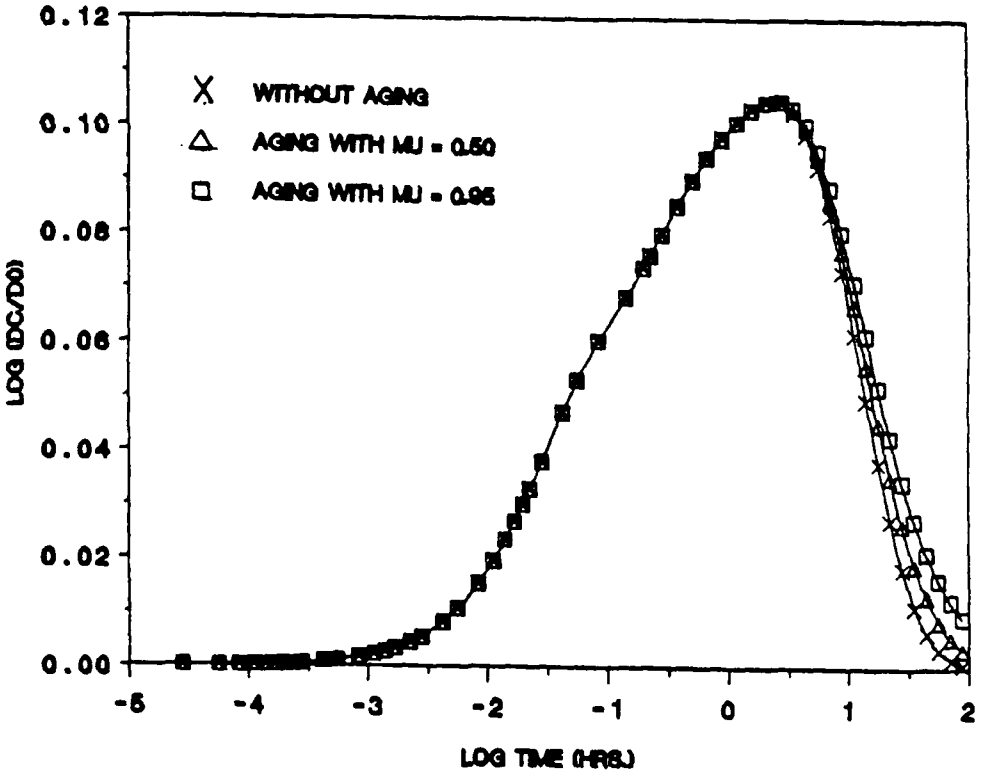

Figure 2[illegible] Effect of Physical Aging on the Diffusion Coefficient for Polystyrene.

of this coupling on the viscoelastic response and moisture diffusion within the adhesive layer of a butt joint was investigated by using the program NOVA. The specimen geometry and finite element discretization are shown in Figs. 21 and 22, respectively. A uniform axial displacement of 0.1 mm is applied at the end of the joint and is held constant with time. The adherends are made of aluminum and the adhesive used is polystyrene. The various material properties are listed in Tables 4 and 5. The selection of polystyrene as an adhesive was prompted by the fact that it is one of the few polymeric materials that have their viscoelastic properties and diffusion parameters adequately documented. The normalized moisture concentration at the free edge of the adhesive layer is unity, and the initial concentration throughout the adhesive layer is zero. The tests are conducted at the reference temperature of 50°C.

Figure 23 shows the moisture concentration profiles within the adhesive layer at three different times when there is no coupling. In this case the diffusion coefficient remains constant with time, that is, $D = D_0$. Figure 24 shows the moisture concentration profiles for the case where there is viscoelastic coupling only, that is, when the diffusion coefficient depends on the transient component of the dilatational strain. Figure 25 depicts the case where there is full coupling, that is, the diffusion coefficient is a function of the dilatational strain and the moisture concentration at any given point in the adhesive. Conversely, the viscoelastic shift factor is now a function of the dilatational strain and the moisture concentration. Figure 26 presents the results for each of these three cases for comparison at time t = 8 hours. From these figures it is evident that

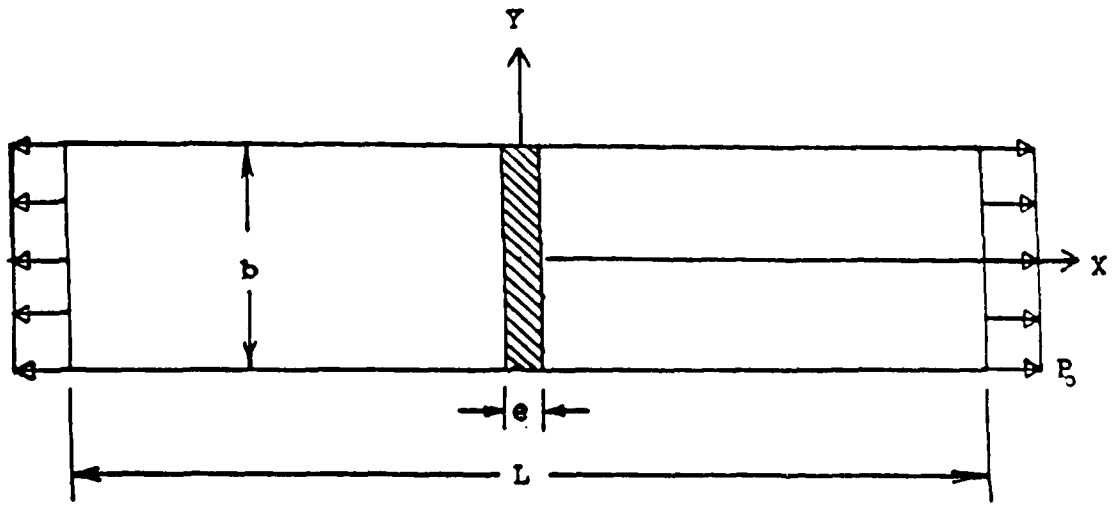

Figure 21 Specimen Geometry and Boundary Conditions for the Analysis of a Butt Joint (L = 200.5, b = 30.0, e = 0.25, all dimensions in mm., Applied Stress = 10 MPa.).

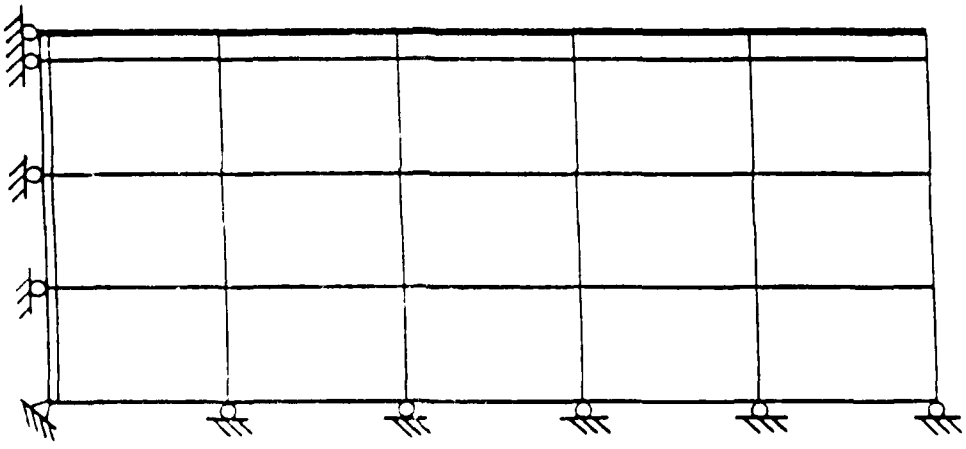

Figure 22 Finite Element Discretization and Boundary Conditions for the Analysis of a Butt Joint.

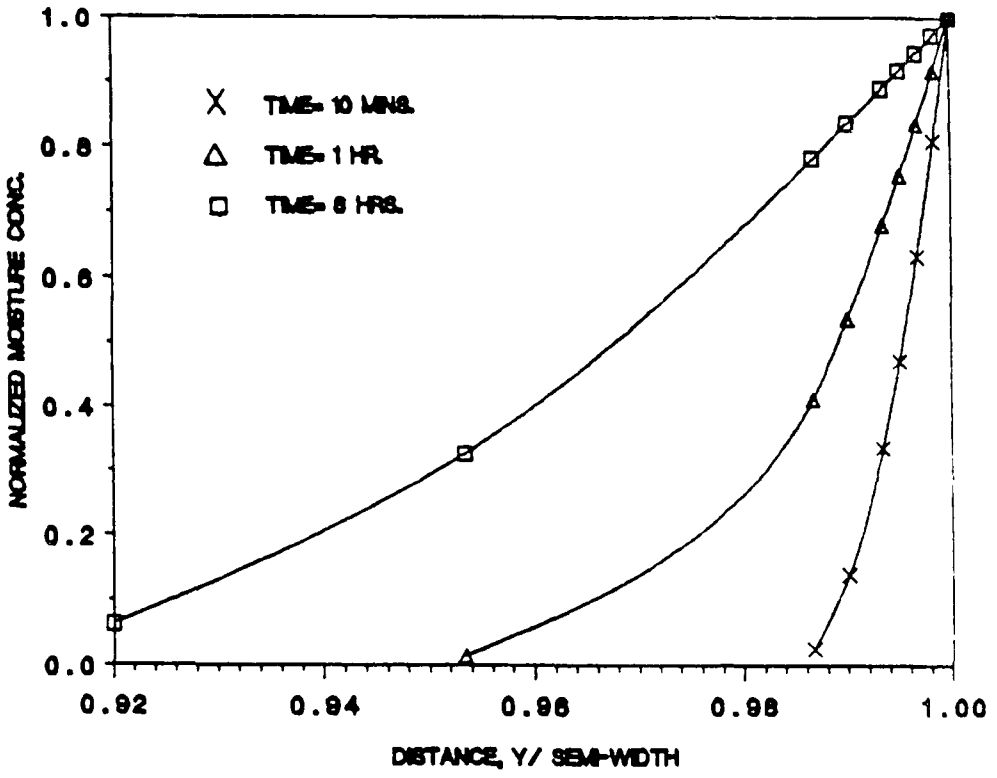

Figure 23 Moisture Profiles Within the Adhesive When There Is No Coupling.

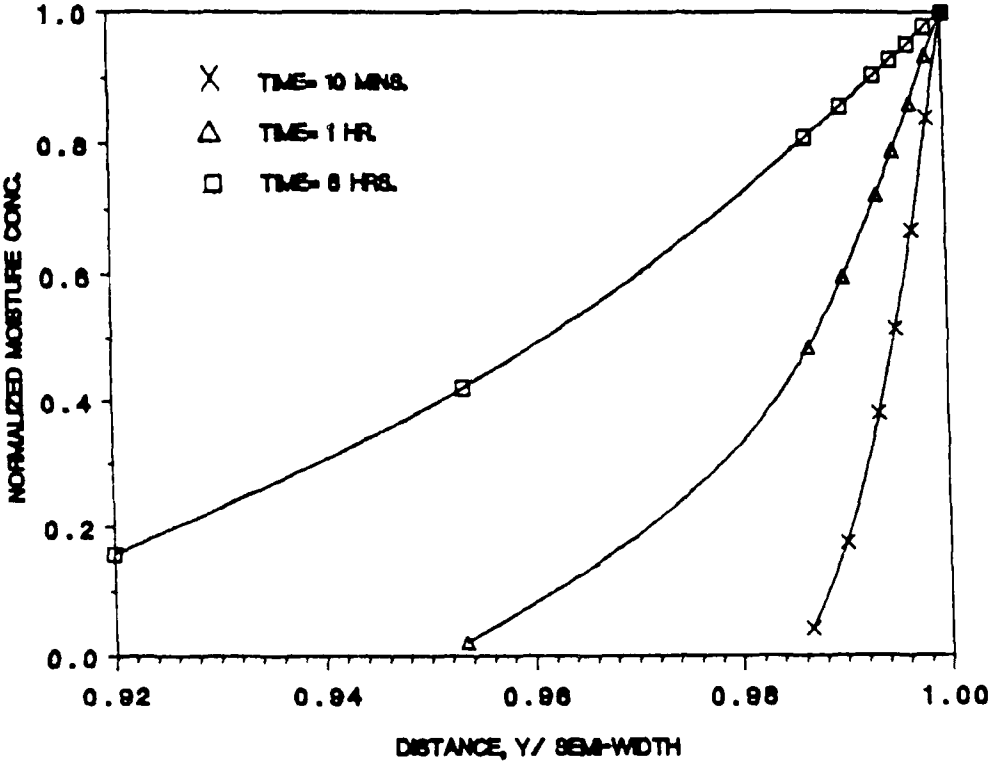

Figure 24 Moisture Profiles Within the Adhesive For Only Viscoelastic Coupling.

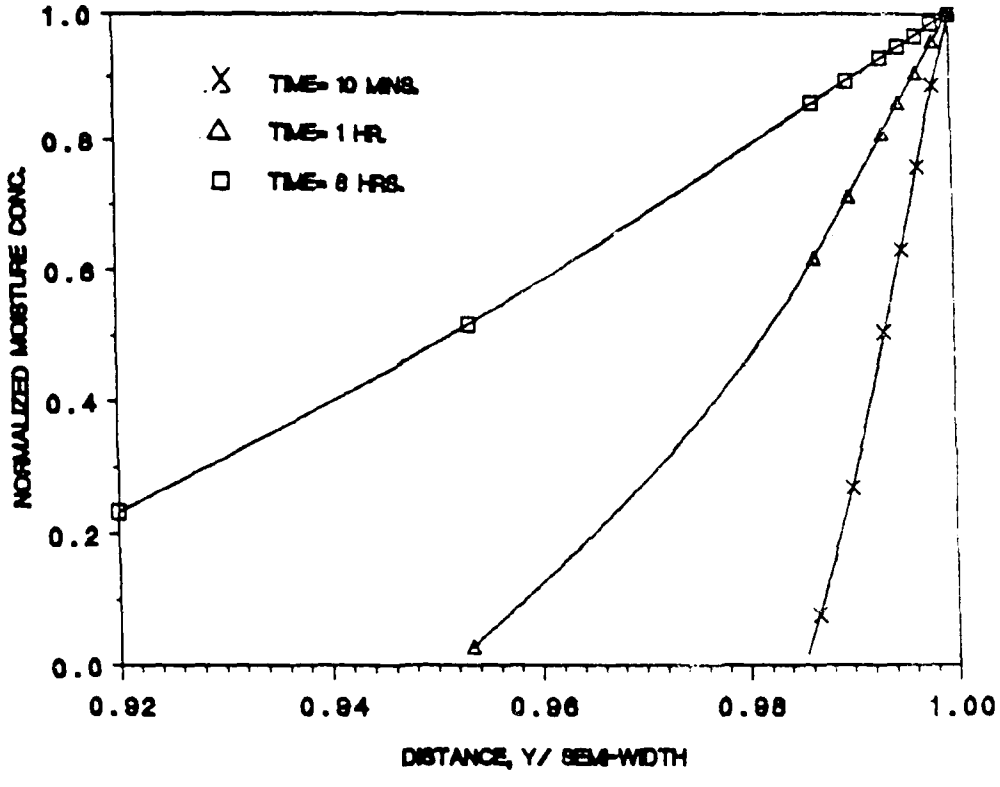

Figure 35 Moisture Profiles Within the Adhesive For Viscoelastic and Moisture Coupling.

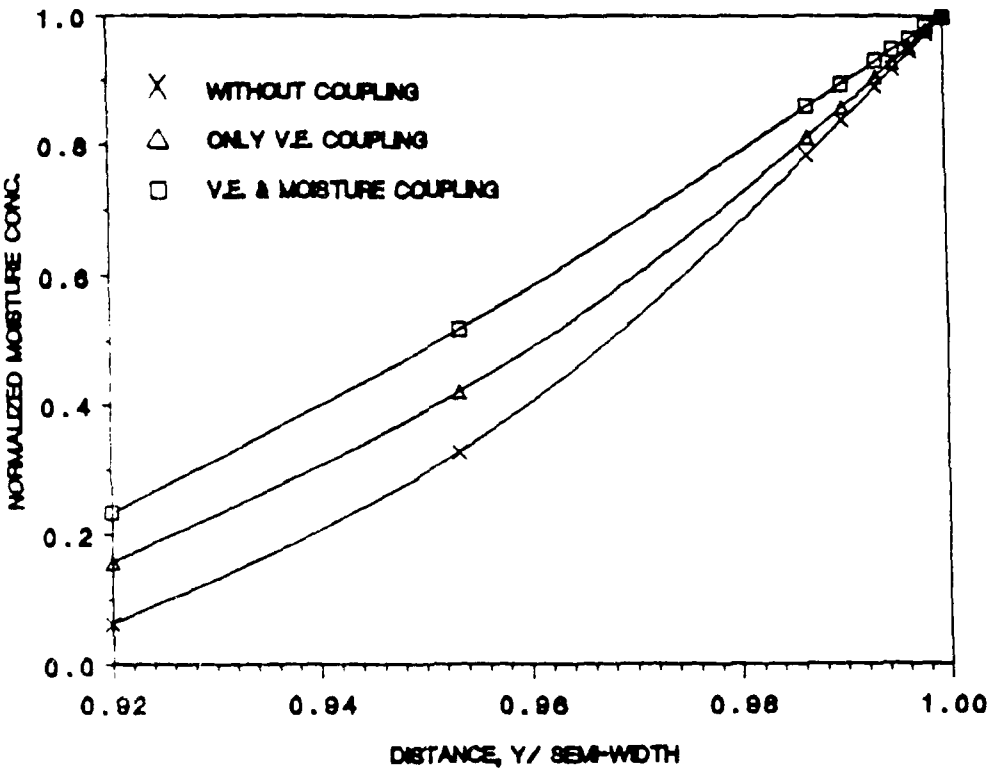

Figure 26 Influence of Coupling on Moisture Profiles at Time = 8 Hours.

Table 5. Properties for Elastic Analysis of a Butt Joint.

Materials	E(MPa)	ν
Steel	2.07×10^5	0.29
Aluminum	0.7×10^5	0.33
Eponal	5.8×10^3	0.33
Rigid Epoxy	2.2×10^3	0.33

the effect of coupling is to accelerate moisture diffusion in the adhesive. The mechanically induced dilatation together with the swelling due to moisture sorption results in a higher free volume fraction within the adhesive which, according to Eq. (3.9), causes diffusion to proceed faster over the same period of time. It is to be noted that in Fig. 26 the curves become less concave as the coupling increases, which is in good agreement with the results published in [20].

Figures 27 to 30 show the variation of the stresses and strains with time within the adhesive layer in the butt joint when there is no coupling due to moisture induced swelling. Mathematically, this implies that $\gamma = 0$ in Eq. (3.8) and (3.11). From Figs. 27 and 28 it is evident that the stresses do not relax significantly over the time period of the analysis. This is because the elastic adherend acts as a spring causing the adhesive to creep even though the joint end displacement remains fixed. However, there is a slight relaxation in the normal stress as one moves towards the center of the bond. The large increase in the strains, as shown in Figs. 29 and 30, is due to the creep caused by the strain recovery in the elastic adherend. This observation is supported by Fig. 31 which shows that the normal strain in the adherend immediately adjacent to the interface undergoes significant reduction with time. The decrease in the adherend normal stress, as shown in Fig. 32, reflects the concurrent stress relaxation that occurs in the adhesive and triggers the strain recovery in the adherend.

Figures 33 to 36 show the effect of moisture induced swelling on the viscoelastic stresses and strains in the adhesive layer. Mathematically, this means γ has a nonzero value in Eqs. (3.8) and

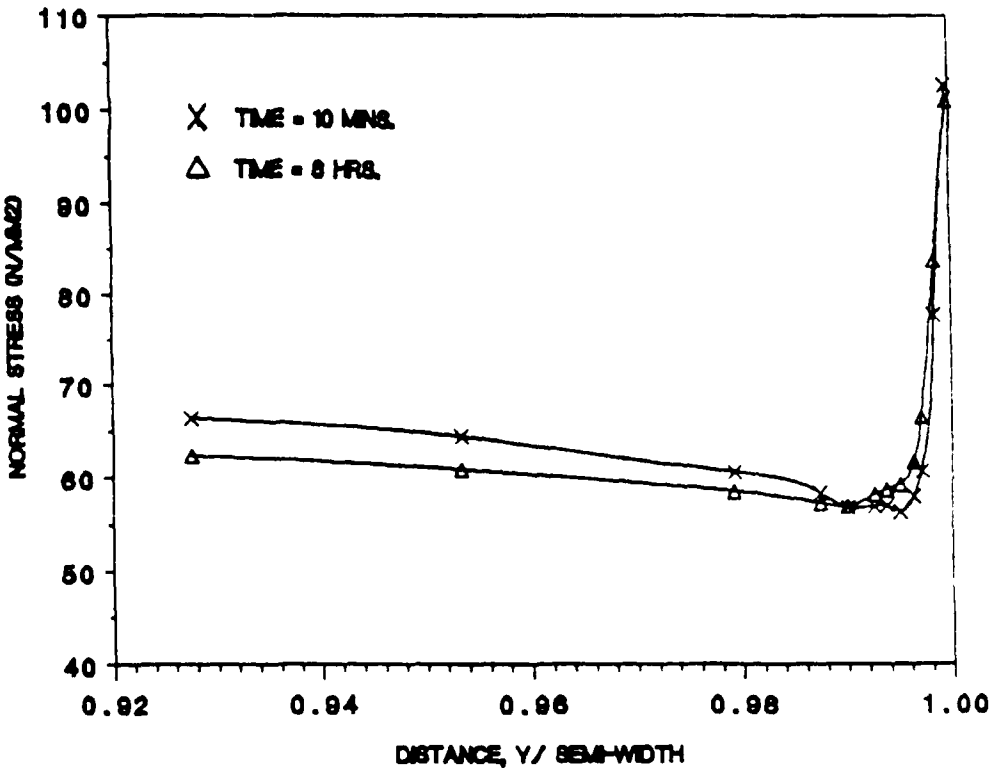

Figure 7 / Variation of Normal Stress in the Adhesive With Time For Viscoelastic Coupling.

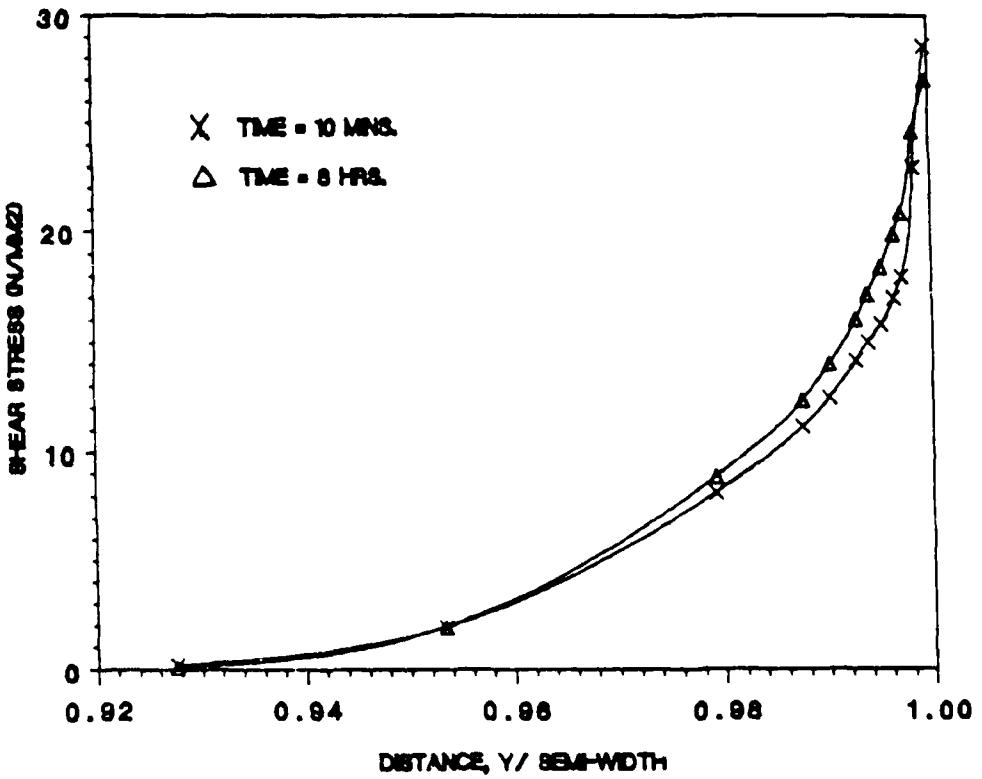

Figure 28 Variation of Shear Stress in the Adhesive With Time For Viscoelastic Coupling.

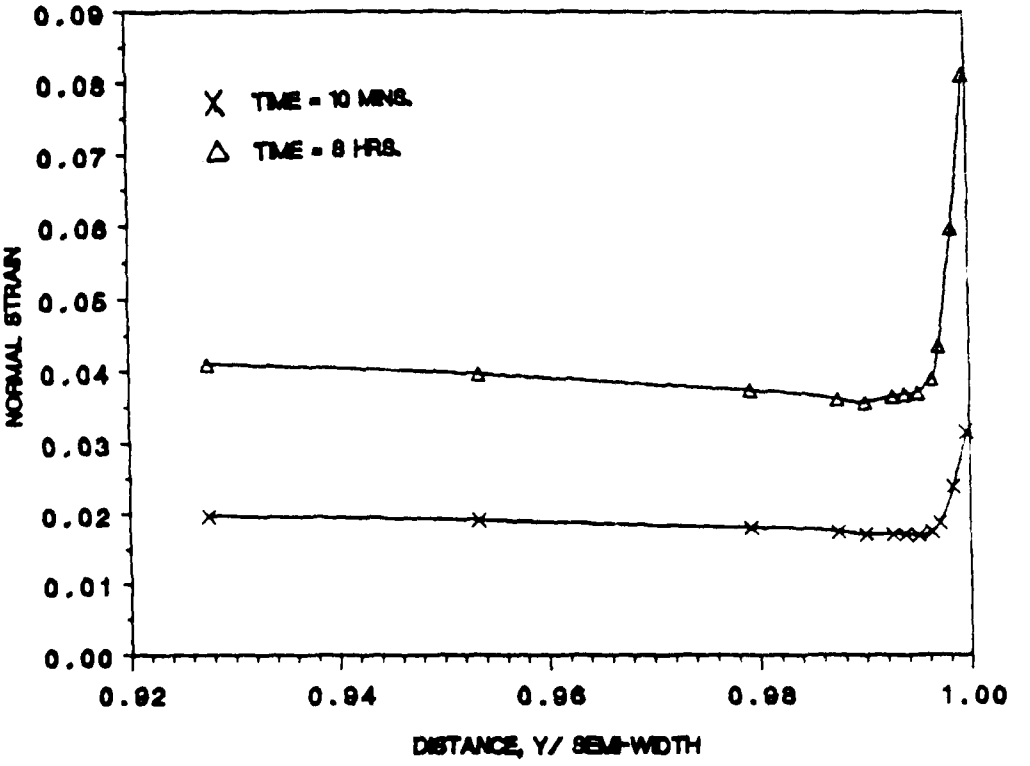

Figure 29 Variation of Normal Strain in the Adhesive With Time For Viscoelastic Coupling.

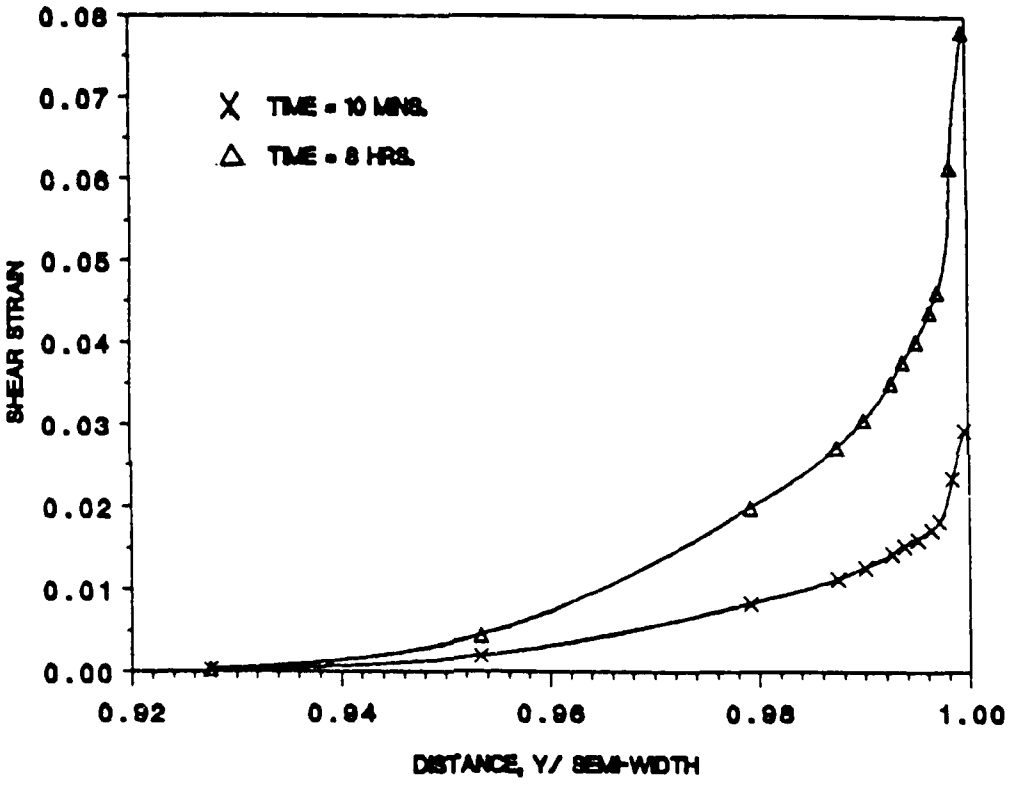

Figure 30 Variation of Shear Strain in the Adhesive With Time For Viscoelastic Coupling.

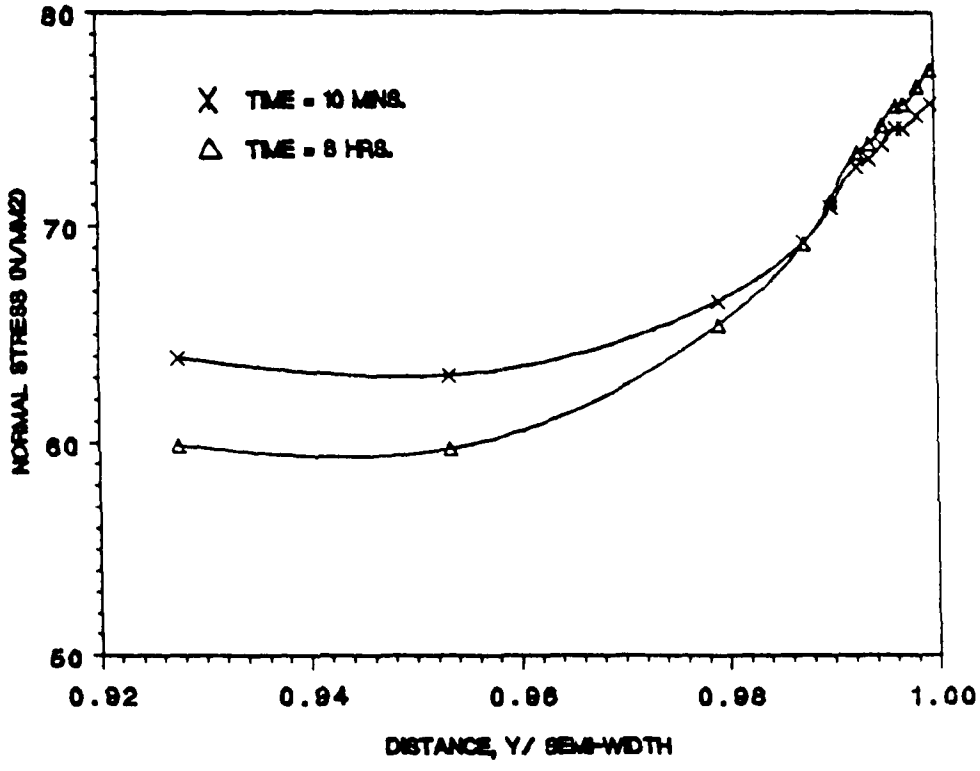

Figure 21 Variation of Normal Stress in the Adherend With Time For Viscoelastic Coupling.

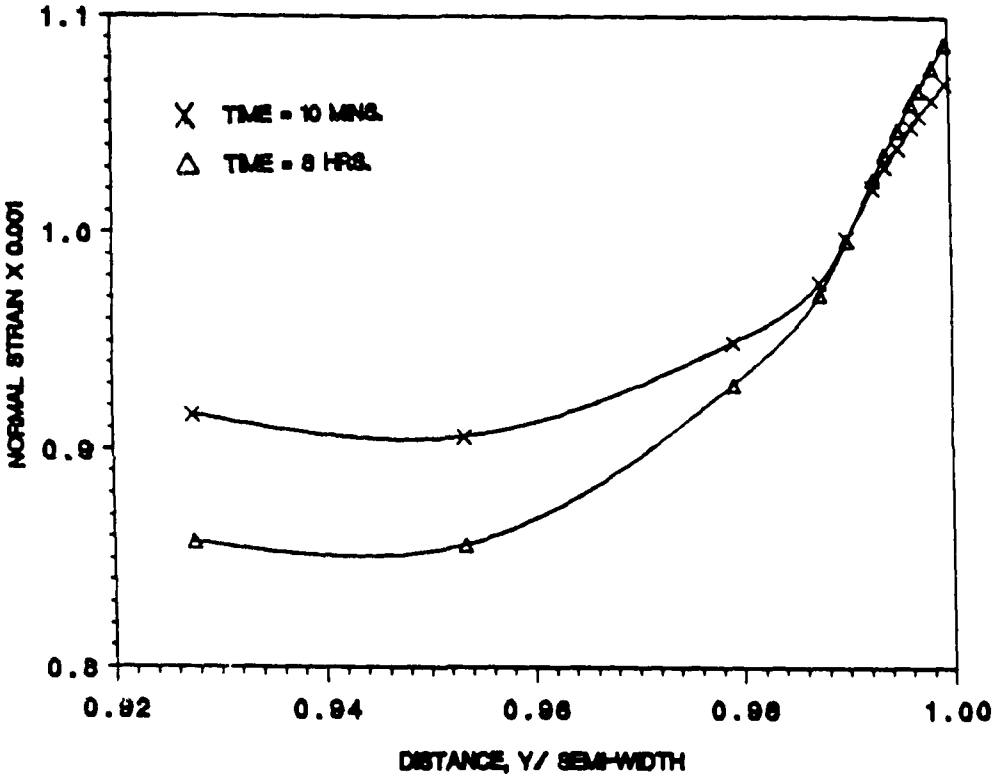

Figure 32 Variation of Normal Strain in the Adherend With Time For Viscoelastic Coupling.

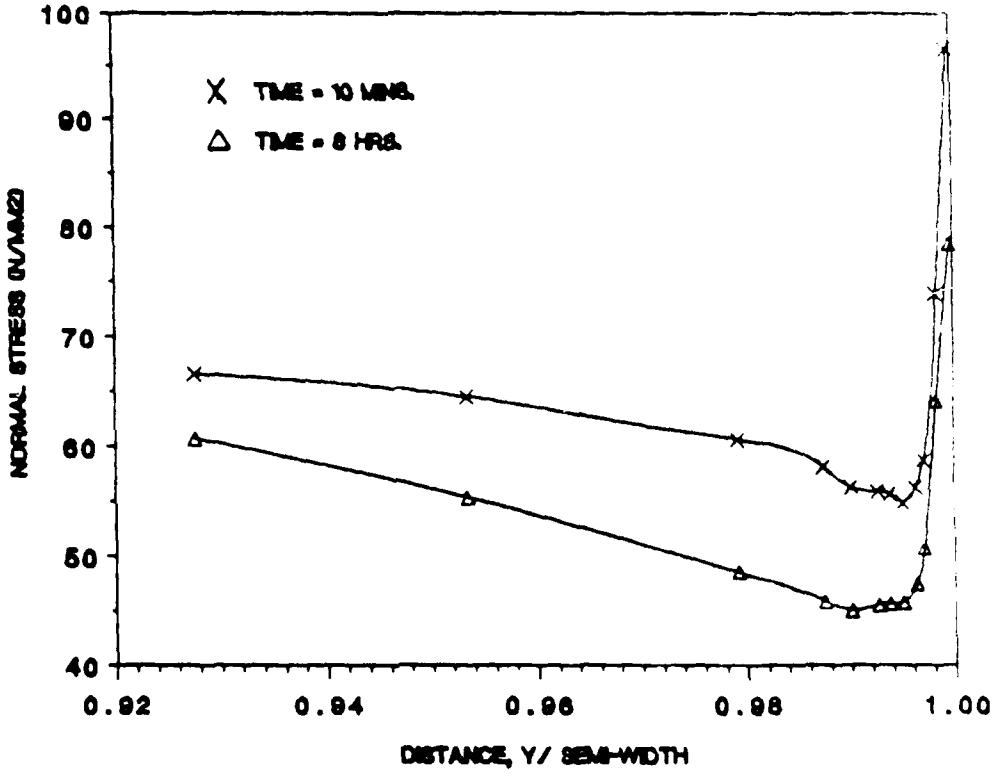

Figure . Variation of Normal Stress in the Adhesive With Time For Viscoelastic and Moisture Coupling.

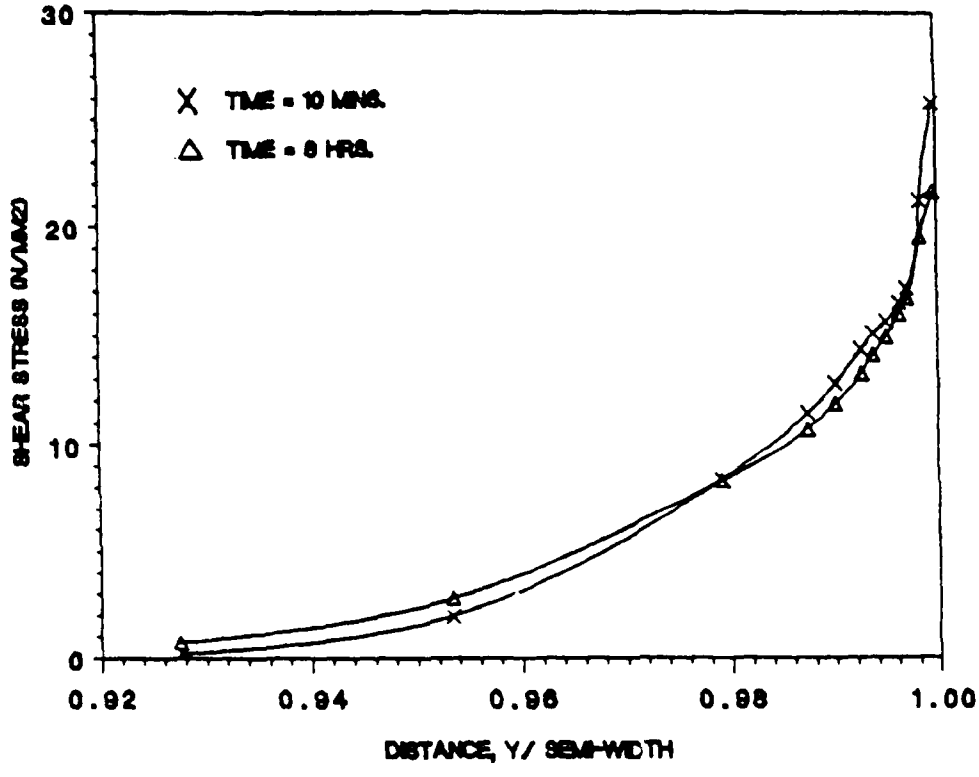

Figure 34 Variation of Shear Stress in the Adhesive With Time For Viscoelastic and Moisture Coupling.

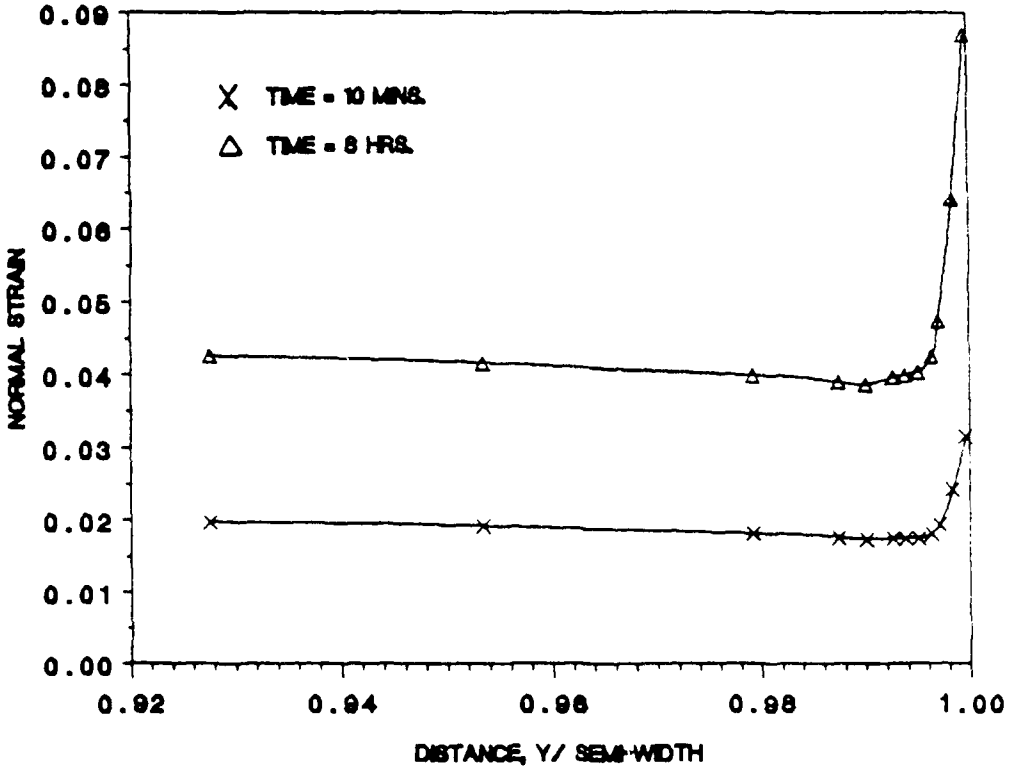

Figure 5.5 Variation of Normal Strain in the Adhesive With Time For Viscoelastic and Moisture Coupling.

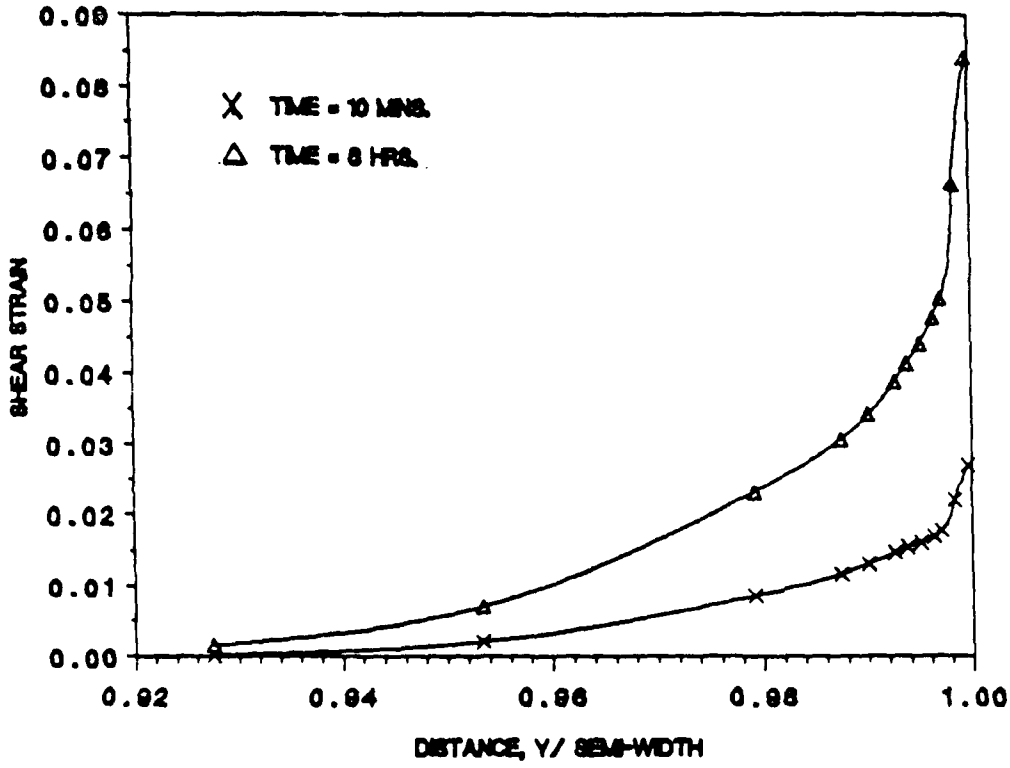

Figure 36 Variation of Shear Strain in the Adhesive With Time For Viscoelastic and Moisture Coupling.

(3.11). The actual value of γ selected for this study is 0.001. For this value of γ, the moisture absorbed causes large swelling strains within the adhesive, which increase in magnitude as the diffusion progresses. This moisture induced swelling strain causes a reduction in the mechanically induced normal strain and hence a lower value for the normal stress in the adhesive. This effect can be observed in Fig. 33 where progressive swelling has caused a 25% reduction in the peak normal stress over a period of 8 hours. It is interesting to note that the difference between the two stress curves diminishes as one moves towards the center of the bond. This behavior is expected since there is very little moisture near the center of the bond and so the stress reduction is primarily due to viscoelastic relaxation. The large increase in the adhesive strains, as seen in Figs. 35 and 36, is due to the adherend acting as a elastic spring.

Figure 37 shows the influence of the moisture coefficient γ, on the normal stress in the adhesive layer after eight hours of sorption. As can be seen, the swelling induced for $\gamma = 0.001$ results in a significantly lower normal stress near the free edge as compared to the case where $\gamma = 0$. Away from the free edge, the two stress curves appear to merge as one moves towards the interior of the bond. This is because the low moisture concentrations present in the bond interior is insufficient to cause any significant reduction in the normal stress due to swelling.

4.5 Delayed Failure of a Butt Joint

The theory presented in Secs. 3.3 and 3.4 was applied to predict viscoelastic creep failure within the adhesive in a butt joint. The specimen geometry and the finite element discretization are the same as

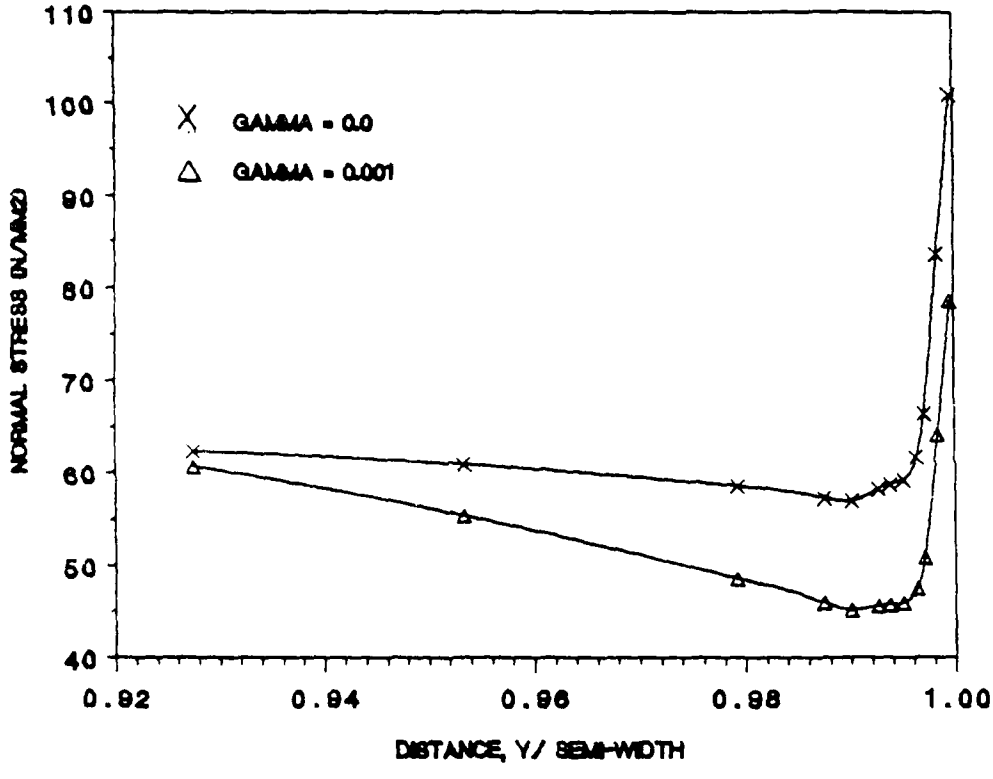

Figure 37 Influence of Moisture Coefficient on Adhesive Normal Stress at Time = 8 Hours.

shown in Figs. 21 and 22, respectively. The adherend is made of aluminum and its material properties are given in Table 5. The adhesive used is FM-73 and its tensile creep compliance is listed in Table 3. The failure parameter (R) for FM-73, also known as the resilience, was obtained by computing the area under the stress-strain curve presented in [24]. This procedure yielded a value of the resilience as 1.3 $N.mm/mm^3$. Note that the area under the visco-plastic yield plateau was not included in computing the value of R. According to the Reiner-Weisenberg theory, failure occurs when the stored energy per unit volume in the body reaches the resilience R, for the material. Using this postulate as a failure criterion, NCV4 was utilized to predict failure in the adhesive layer of the butt joint subject to a constant uniaxial tension. The influence of applied stress level on delayed failure was studied by using a stress level of 69, 60, and 54 MPa respectively. In all three cases, failure was initiated in the adhesive element located right at the free-edge and immediately adjacent to the interface. It was also observed that the direction of the plane of failure was always inclined at an angle of 18°, counter-clockwise to the x-axis. Since the direction of failure coincides with the direction of principal stress, it is evident that a multiaxial state of stress exists near the free edge, even though the applied stress is uniaxial. Figure 38 shows the variation of normal (or creep) strain with time at 30 C for the element in which failure is first initiated. The right hand termination point on the curves indicate the point at which failure occured. It is observed that for an applied stress level of 69 MPa, the time to failure (t_F) is 1.5 secs. In other words, for this stress level, failure occurs almost instantaneously. For an applied stress of 60 MPa, t_F increases

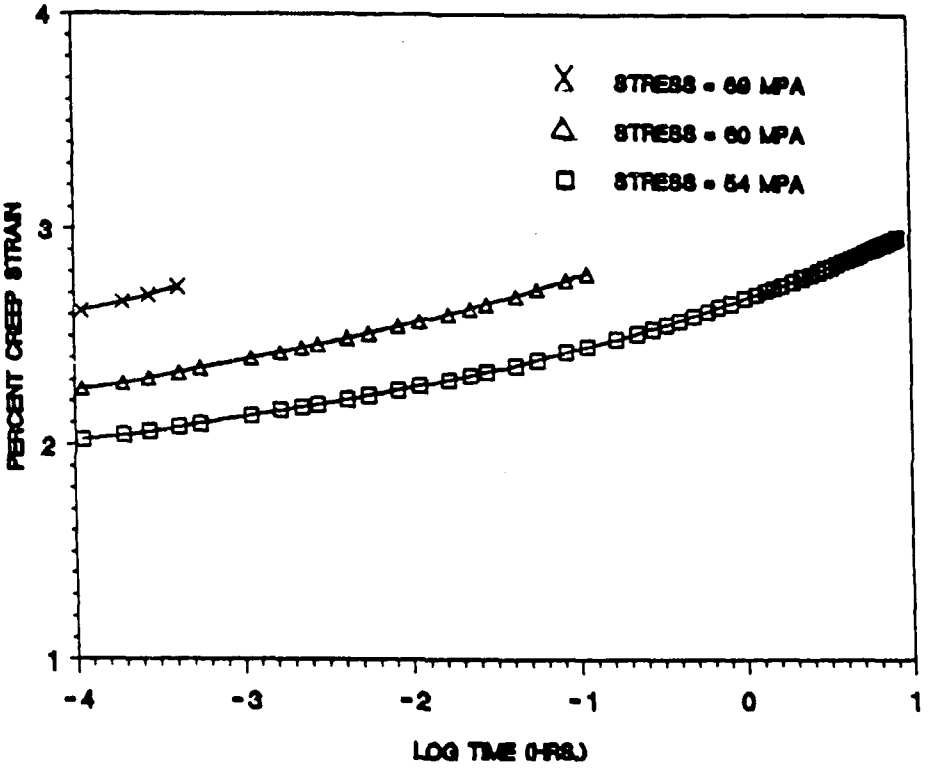

Figure 38 Creep Strain in FM-73 for Different Applied Stress Levels.

to 400 secs. Reducing the applied stress to 54 MPa results in a time to failure of approximately 10 hours. These results are qualitatively in good agreement with the results presented by Bruller [6] for PMMA.

From the above observations it is clearly evident that for viscoelastic polymers like FM-73, the time to failure depends strongly on the applied stress level. Figure 39 shows the evolution of stored energy with time for different stress levels. For very high applied stress levels, almost all the strain energy is conserved as stored energy and failure occurs almost immediately. For intermediate levels of applied stress, viscoelastic creep causes a part of the strain energy to be dissipated. As a result, only a fraction of the total strain energy is conserved as stored energy. Consequently, the stored energy builds up slowly, analogous to a "leaking vessel", resulting in delayed failure. For an applied stress level that is below a certain threshold value for a given material, the dissipated energy may constitute a large fraction of the total strain energy. In that case, the stored energy would increase too slowly to exceed the resilience of the material over any realistic length of time, and hence there would be no failure even if the applied stress acts indefinitely.

5. SUMMARY AND CONCLUSIONS

5.1 General Summary

The adhesive layer is modeled using Schapery's nonlinear single integral constitutive law for uniaxial and multiaxial stress states. The effect of temperature and stress level on the viscoelastic response is taken into account by a nonlinear shift factor definition. Penetrant sorption is accounted for by a nonlinear Fickean diffusion model in which the diffusion coefficient is dependent on the temperature,

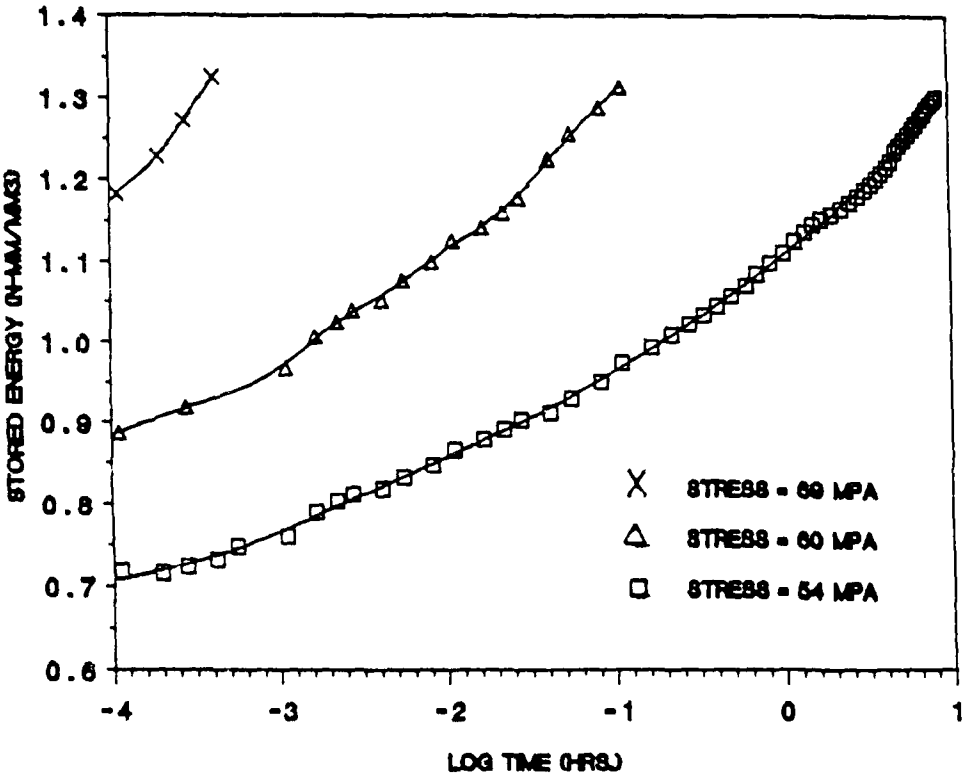

Figure 39 Stored Energy in FM-73 for Different Applied Stress Levels.

penetrant concentration, and the dilatational strain. A delayed failure criterion based on the Reiner-Weisenberg failure theory has also been implemented in the finite element code. The program is validated by comparing the present results with analytical and experimental results available in the literature. The program capability has been extended to account for laminated composite adherends and adhesives with a time dependent Poisson's ratio. In general, the computer program NOVA, is believed to provide accurate predictions over a wide range of specimen geometries, external loads, and environmental conditions.

5.2 *Conclusions*

The results presented in Section 4 underscore the importance of modeling the adhesive in a bonded joint as a viscoelastic material. This allows the analyst to predict the large increments in adhesive strains that occur with time and cannot be predicted by a purely elastic analysis. Furthermore, other events (such as moisture diffusion and delayed failure), that are highly relevant for bonded joint analysis, cannot be accurately predicted unless viscoelasticity is taken into account. At high stress levels, nonlinear viscoelastic effects can produce creep strains that are significantly larger than the linear viscoelastic predictions and such effects, therefore, should be accounted for. The effect of change in Poisson's ratio with time in some polymers have a significant bearing on the final response and must be taken into account in order to obtain accurate results.

REFERENCES

1. J. N. Reddy and S. Roy, "Finite Element Analysis of Adhesively Bonded Joints," Report No. VPI-E-85.18, Department of Engineering Science and Mechanics, VPI&SU, Blacksburg, VA, 1985.

2. S. Roy and J. N. Reddy, "Nonlinear Viscoelastic Analysis of Adhesively Bonded Joints," Report No. VPI-E-86.28, Department of Engineering Science and Mechanics, Virginia Polytechnic Institute and State University, Blacksburg VA, 1986.

3. P. M. Nagdhi and S. A. Murch,"On the Mechanical Behavior of Viscoelastic-Plastic Solids," Journal of Applied Mechanics, Vol. 30, p. 327, 1963.

4. M. J. Crochet, "Symmetric Deformations of Viscoelastic Plastic Cylinders," Journal of Applied Mechanics, Vol. 33, pp. 327-334, 1966.

5. M. Reiner and K. Weisenberg, "A Thermodynamic Theory of the Strength of Materials," Rheology Leaflet No., Vol. 10, pp. 12-20, 1939.

6. O. S. Bruller, "On the Damage Energy of Polymers in Creep," Polymer Engineering and Science, Vol. 18, No. 1, 1978.

7. Clement Hiel, A. H. Cardon, and H. F. Brinson, "The Nonlinear Viscoelastic Response of Resin Matrix Composite Laminates," Report No. VPI-E-83-6, Department of Engineering Science and Mechanics, VPI&SU, Blacksburg, VA, 1983.

8. Y. Weitsman, "Stresses in Adhesive Joints Due to Moisture and Temperature," J. Composite Materials, Vol. 11, p. 368, 1977.

9. Y. Weitsman, "Interfacial Stresses in Viscoelastic Adhesive-Layers Due to Moisture Sorption," Int. J. Solids Structures, Vol. 15, pp. 701-713, 1979.

10. F. E. L. Tobing, M. S. Shephard and S. S. Sternstein, "Finite Element Analysis of Moisture Effects in Graphite-Epoxy Composites," Computers & Structures, Vol. 16, pp. 457-469, 1983.

11. G. Yaniv and O. Ishai, "Hygrothermal Effects on Stresses and Deformations in a Bonded Fiber-Reinforced Plastic/Aluminum System," Composites Technology Review, Vol. 6, No. 2, pp. 63-73, 1984.

12. D. R. Lefebvre, T. C. Ward, D. A. Dillard, H. F. Brinson, "A Nonlinear Constitutive Behavior for Diffusion in Polymers," Report No. VPI-E-87-2, CAS/ESM-87-1, Virginia Polytechnic Institute and State University, Blacksburg, VA, 1987.

13. R. A. Schapery, Further Development of a Thermodynamic Constitutive Theory: Stress Formulation, A&S Report No. 69-2, Purdue University, W. Lafayette, 1969.

14. C. Hiel, A. H. Cardon, and H. F. Brinson, "The Nonlinear Viscoelastic Response of Resin Matrix Composite Laminates," Department of Engineering Science and Mechanics, Virginia Polytechnic Institute and State University, Blacksburg, VA, 1983.

15. W. G. Knauss and I. J. Emri, Nonlinear Viscoelasticity Based on Free Volume Considerations, Computers and Structures, vol. 13, pp. 123-128, 1981.

16. R. A. Schapery, "On the Characterization of Nonlinear Viscoelastic Materials," Polymer Engineering and Science, Vol. 9, No. 4, p. 295. 1969.

17. J. N. Reddy, An Introduction to the Finite Element Method, McGraw-Hill, New York, 1984.

18. W. J. Renton and J. R. Vinson, "On the Behavior of Bonded Joints in Composite Material Structures," Engineering Fracture Mech, Vol. 7, p. 41, 1975.

19. J. A. Harris and R. D. Adams, "Strength Prediction of Bonded Single Lap Joints by Non-Linear Finite Element Methods," International Journal of Adhesion and Adhesives, Vol. 4, No. 2, p. 65, 1984.

20. J. Crank, The Mathematics of Diffusion, Second Edition, Clarendon Press, Oxford, 1975.

21. G. Levita and T. L. Smith, "Effect of Tensile Strain, Time, and Temperature on Gas Transport in Biaxially Oriented Polystyrene," Polymer Engineering and Science, Vol. 21, No. 14, p. 536, 1981.

22. J. D. Ferry, Viscoelastic Properties of Polymers, 3rd Edition, Wiley, New York, 1980.

23. L. C. E. Struik, Physical Aging in Amorphous Polymers and Other Materials, Elsevier, 1978.

24. G. Dolev and O. Ishai, Mechanical Characterization of Adhesive Layer In-Situ and as Bulk Material, J. Adhesion, Vol. 12, pp. 283-294, 1981.

Acknowledgements.

The authors acknowledge the many discussions with Mr. D. R. Lefebvre, Professors T. C. Ward and H. F. Brinson and Dr. D. A. Dillard on the subject of diffusion and failure models. It is also a pleasure to acknowled e the skilful typing of the long manuscript by Mrs. Vanessa McCoy. The support and encouragement of this research by Dr. Larry Peebles, Jr. (ONR) is gratefully acknowledged.


ED
8